# Advanced Architectures and Control Concepts for

# MORE MICROGRIDS

**Contract No:** PL**019864**

WORK PACKAGE A

DA3: Advanced Optimisation for Domestic CHP

Final Version

February 25, 2008

# Document Information

**Deliverable:** DA3

**Title**: Advanced Optimisation for Domestic CHP

**Date**: 25-February-2008

**Worpackage(s)**: WPA: Design of Micro-Source and Load Controllers for Efficient Integration

**Task(s)**: TA1. Requirements for various DGs in supporting Microgrid operation


| | | |
|---|---|---|
| **Coordination:** | Nick Jenkins | Nick.Jenkins@manchester.ac.uk |
| **Authors**: | T Sulka | Tomasz.Sulka@manchester.ac.uk |
| | M. Chaudry | Modassar.Chaudry@manchester.ac.uk |
| | J.B. Ekanayake | Janaka.Ekanayake-2@manchester.ac.uk |


**Access**:

- _ Project Consortium
- _ European Commission
- X PUBLIC

**Status**:

- _ For Information
- _ Draft Version
- _ Final Version (internal document)
- _ Submission for Approval (deliverable)
- X Final Version

# CONTENTS

*Chapter 1*

# INTRODUCTION

It is anticipated that µCHP will play a leading role in fulfilling future domestic heating requirements while producing electricity simultaneously. A number of different technologies have been developed or are under development for µCHP units with different thermal and electrical conversion efficiencies [2]. For this diverse range of technologies, the thermal conversion efficiency is typically 70 – 80% and the electrical conversion efficiency is around 10 – 25%. Some µCHP units can operate on part-load, where their part-load efficiency is less than their full-load efficiency.

In the Energy White paper [1], µCHP has been recognised as an option that can offer carbon savings, thus a number of support measures to encourage their development is being pursued. According to [2], in the UK the potential market for 0.8 - 1 $kW_e$ / 5 - 6 $kW_{th}$ µCHP units is likely to be between 12,000 - 24,000 $MWh_e$ per annum or approximately 8 million homes. The technology which is currently close to market is based on a Stirling engine.

Under the project “More MicroGirds”, the University of Manchester (UM) will focus on advanced optimisation for domestic µCHP units. The algorithms for the scheduling of these devices was developed to maximise benefits for individual customers while taking into account various operating constraints and conditions, such as desired room and water temperature range at particular times of use, ambient temperature, the characteristics of thermal insulation, and the time varying price of electricity and gas.

In Chapter 2, the basic thermal model of a house was developed. The model was based on the detailed modelling of the characteristics of a dwelling and its occupants. It was shown that the heat demand curve reflects the desired room and water temperature range, ambient temperature and other properties of the dwelling.

In Chapter 3, five possible operating modes for a µCHP unit, where part-loading is possible, are presented. In this study, the characteristics of a house were reflected by its heat and electricity demand profiles.

The first part of Chapter 4 describes the development of the temperature control strategy for the μCHP unit. The μCHP was controlled to achieve the desired room and water temperature of the dwelling. The work was then extended to carryout an economic optimisation of the μCHP unit. A similar optimisation study was carried out under the MicroGrid project [3], in that study it was assumed that the μCHP unit was operating with part-loading at the same efficiency as its full-load efficiency. The work discussed in this report is based on a Stirling Engine type μCHP unit where only full-load and idling (or off) conditions are possible. Cost optimisation studies were extended to a μCHP unit which is connected to two houses. It was assumed that both thermal and electrical networks between the houses are interconnected. Different occupancy patterns for the two houses were considered.

Chapter 5 illustrates a case study based on an estate having a large number of dwellings with μCHP units.

*Chapter 2*

# MODELLING A SINGLE HOUSE WITH A *μ*CHP UNIT

## 2.1 List of Symbol

| | |
|---|---|
| $\theta_H$ | Temperature inside the house (K) |
| $\theta_T$ | Hot water temperature (K) |
| $\theta_{H,ref}$ | Space reference temperature (K) |
| $\theta_{T,ref}$ | Hot water reference temperature (K) |
| $\theta_A$ | Outside temperature (K) |
| $C_H$ | Rate of change of specific thermal capacity of the house (kW/K) |
| $C_T$ | Rate of change of specific thermal capacity of water (kW/K) |
| $L_H$ | Heat loss factor for the house (kW/K) |
| $L_T$ | Heat loss factor for the hot water tank (kW/K) |
| $Q_C$ | Heat output of the μCHP unit (kW) |
| $Q_H$ | Heat consumption of the house (kW) |
| $Q_T$ | Heat consumption of the hot water tank (kW) |
| $D_T$ | Hot water demand (kW) |

## 2.2 Thermal behaviour of an enclosed volume [1]

Figure 1 shows an enclosed volume of *V* ($m^3$) which is covered by a material of thermal resistance R ($m^2$K/kW).

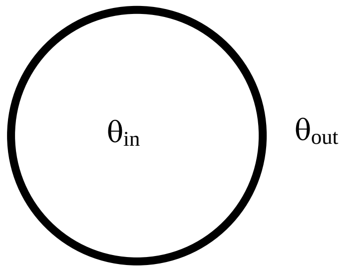

Figure 1: Enclosed volume

It was assumed that the heat associated with the enclosed volume is *Q* and after a time $\Delta t$, the temperature difference in the volume is $\Delta\theta$.

Thermal energy associated with the volume:

$$Q \times \Delta t = V\rho c \times \Delta\theta$$

Where ρ is the density (kg/m3) and *c* is the specific thermal capacity (J/kgK)

$$\therefore Q = \frac{V\rho c}{\Delta t} \times \Delta\theta = C \times \frac{\Delta\theta}{\Delta t} \qquad (1.1)$$

Assuming that the surrounding structure dissipates heat to the environment without any time delay, the heat lost, $Q_L$, in time Δt is given by:

$$Q_L = \frac{A}{R} \times (\theta_{in} - \theta_{out}) = L \times (\theta_{in} - \theta_{out}) \qquad (1.2)$$

Where *A* is the surface area of the surrounding structure.

## 2.3 House with a μCHP units and a Hot Water Tank (HWT)

Figure 2 shows the house considered for the study. It was assumed that the μCHP unit is a Sterling Engine type where only full-load and idling modes of operations are possible.

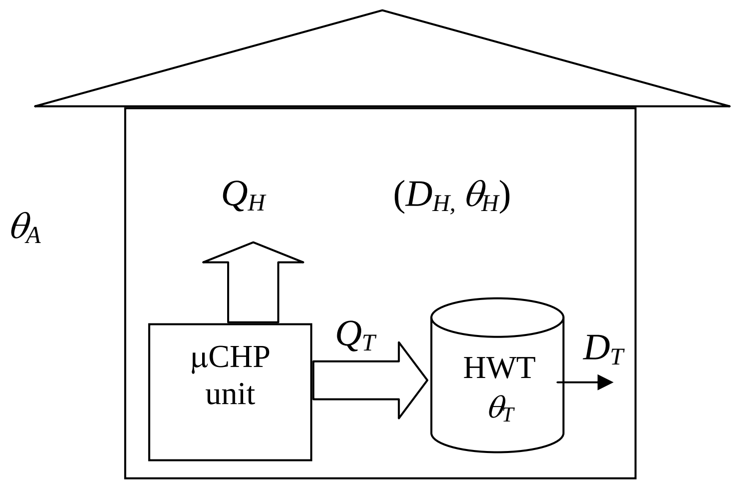


Figure 2: Simplified diagram of the house

For a time period Δt, the following were assumed:

- Temperature inside the house changes from *$\theta_H(i)$* to *$\theta_H(i+1)$*
- Temperature inside the tank changes from *$\theta_T(i)$* to *$\theta_T(i+1)$*
- Outside temperature remains constant at $\theta_A$
- The hot water demand, $D_T$, is a constant
- Heat loss is governed by the average temperature within the time period Δt

Furthermore, it was assumed that the heat produced by occupants, appliances and heat loss or gain due to disturbances (such as opening a window, a fridge, etc.) are negligible[1].

*When the μCHP is ON:*

The heat produced by the μCHP unit is used for space heating ($Q_H$) and for hot water heating ($Q_T$).

For the thermal equilibrium of the house, from equations (1.1) and (1.2)

$$Q_H = C_H \frac{[\theta_H(i+1) - \theta_H(i)]}{\Delta t} + L_H \left[ \frac{\theta_H(i+1) + \theta_H(i)}{2} - \theta_A \right]$$

$$\therefore \left[ \frac{C_H}{\Delta t} + \frac{L_H}{2} \right] \times \theta_H(i+1) - \left[ \frac{C_H}{\Delta t} - \frac{L_H}{2} \right] \times \theta_H(i) - Q_H - L_H \theta_A = 0 \qquad (1.3)$$

For the HWT, assuming that the average temperature inside the house is approximately equal to $\theta_H(i)$,

$$Q_T = C_T \frac{[\theta_T(i+1) - \theta_T(i)]}{\Delta t} + L_T \left[ \frac{\theta_T(i+1) + \theta_T(i)}{2} - \theta_H(i) \right] + D_T$$

$$\left[ \frac{C_T}{\Delta t} + \frac{L_T}{2} \right] \times \theta_T(i+1) - \left[ \frac{C_T}{\Delta t} - \frac{L_T}{2} \right] \times \theta_T(i) - Q_T - L_T \theta_H(i) + D_T = 0 \qquad (1.4)$$

In matrix form

[1] The heat output from occupants and the appliances including lighting, depends on the occupancy pattern and the occupants activities. This may be in the range of 90 – 190 W at 20°C.

$$\begin{bmatrix}\theta_H(i+1)\\ \theta_T(i+1)\end{bmatrix} = \begin{bmatrix}\mu_H & 0\\ L_T\alpha_T & \mu_T\end{bmatrix}\begin{bmatrix}\theta_H(i)\\ \theta_T(i)\end{bmatrix} + \begin{bmatrix}\alpha_H & 0\\ 0 & \alpha_T\end{bmatrix}\begin{bmatrix}Q_H\\ Q_T\end{bmatrix} + \begin{bmatrix}L_H\alpha_H\theta_A\\ -\alpha_T D_T\end{bmatrix} \qquad (1.5)$$

Where $\mu_H = \left[\frac{C_H}{\Delta t} - \frac{L_H}{2}\right] \Big/ \left[\frac{C_H}{\Delta t} + \frac{L_H}{2}\right]$ and $\alpha_H = 1 \Big/ \left[\frac{C_H}{\Delta t} + \frac{L_H}{2}\right]$

$\mu_T = \left[\frac{C_T}{\Delta t} - \frac{L_T}{2}\right] \Big/ \left[\frac{C_T}{\Delta t} + \frac{L_T}{2}\right]$ and $\alpha_T = 1 \Big/ \left[\frac{C_T}{\Delta t} + \frac{L_T}{2}\right]$

When the μCHP is OFF, $Q_H$ and $Q_T$ in equation (1.5) are zero.

## 2.4 Space and hot water demand of a House - A case study

Table 1 shows the capacity and loss factor for the flat and the hot water tank considered for this case study [4].

Table 1: Heat parameters of the house and HWT

| | Capacity C (kWh/K) | Loss factor L(kW/K) |
|---|---|---|
| Flat | 0.4032 | 0.0669 |
| HWT (150 l) | 0.1680 | 0.0003 |

Assuming that the time step used for simulations is 0.5 hr, the model parameters were calculated:

$\mu_H = 0.9203$ $\alpha_H = 1.1907$ K/kW

$\mu_T = 0.9991$ $\alpha_T = 2.9749$ K/kW

Therefore, when the μCHP is ON, the heat and temperature are related by the following equation:

$$\begin{bmatrix} \theta_H(i+1) \\ \theta_T(i+1) \end{bmatrix} = \begin{bmatrix} 0.9203 & 0 \\ 0.0009 & 0.9991 \end{bmatrix} \begin{bmatrix} \theta_H(i) \\ \theta_T(i) \end{bmatrix} + \begin{bmatrix} 1.1907 & 0 \\ 0 & 2.9749 \end{bmatrix} \begin{bmatrix} Q_H \\ Q_T \end{bmatrix} + \begin{bmatrix} 0.0797\theta_A \\ -2.9749D_T \end{bmatrix} \quad (1.6)$$

The house model given in equation (1.6) was modelled using Matlab. The heat required to drive the space and hot water temperature, $\theta_H(i+1)$ and $\theta_T(i+1)$, towards the references, $H_{ref}$ and $T_{ref}$, shown in Figure 3 was obtained. The hot water demand for a winter weak day shown in Appendix A was used for $D_T$ [5]. Figure 4 shows the demand for the space, hot water and total heating requirement of the house.

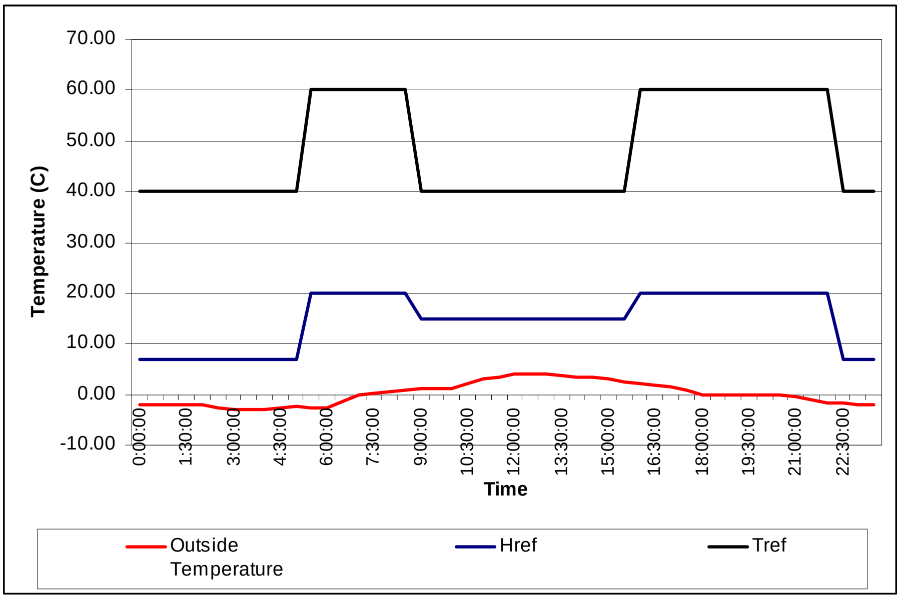


Figure 3: Outside, Space and Hot water reference temperature for a typical winter day

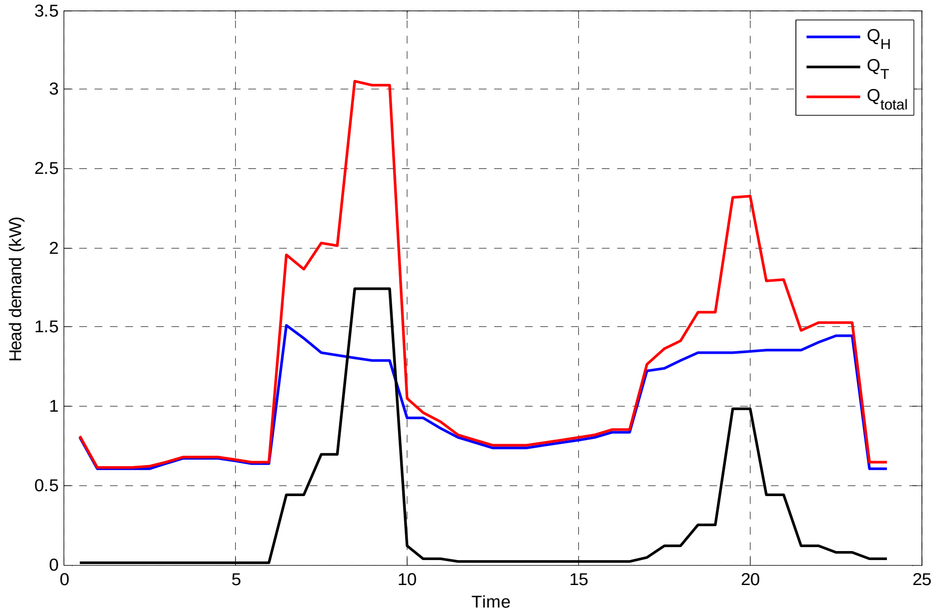


Figure 4: Heat demand for space, hot water and total heating requirement of the house

*Chapter 3*

# CONTROL ALGORITHMS FOR A DEMAND-FOLLOWING µCHP UNIT

## 3.1 List of Symbol

| | |
|---|---|
| $P_e^{out}$ | Electricity demand |
| $P_h^{out}$ | Heat demand |
| $P_e^{in}$ | Electrical power imported from electricity network |
| $P_g^{in}$ | Gas imported from gas network |
| $P_h^{in}$ | Heat imported from district heating system |
| $\alpha$ | The energy carrier: heat, electricity or gas |
| $C_\alpha$ | Cost related to the energy carrier $\alpha$ in monetary units |
| $P_\alpha^{in}$ | Power flowing into the hub input $\alpha$ in power units |
| $a_{\alpha,0}$ | Fixed costs related to $\alpha$ |
| $a_{\alpha,m}$ | Coefficients for demand of $\alpha$ |
| $b_{\alpha,n}$ | Coefficients for delivery of $\alpha$ |

## 3.2 Introduction

Some µCHP units such as the one based on the reciprocating internal combustion engine, can respond to rapid load changes where as other units such as one based on Stirling engines can only operate in discrete modes, full-load and idling (or off). The µCHPs based on fuel cells has a poor load following capability. However the addition of battery storage can help with load following capability. In this chapter a number of control algorithms for a µCHP unit that can load follow are presented. The µCHP unit which operates in discrete mode is investigated in Chapter 4.

## 3.3 Energy Hub model and the cost function

The idea of energy conversion in a hub to meet demand requirements is described in [6]. In this article, a general description of the conversion of different energy carriers to supply domestic demands was described. The hub used for this study is shown in Figure 5. The hub consists of a µCHP unit, Heat Exchanger (HE), electricity, heat and gas inputs, and electricity and heat outputs. The gas to electricity conversion efficiency of the µCHP, $\eta_e$, is 0.35, and the gas to heat conversion efficiency, $\eta_{th}$, is 0.40. The efficiency of the HE, $\eta_H$, is 0.99. The power conversion for the hub is given by:

$$\begin{bmatrix} P_e^{out} \\ P_h^{out} \end{bmatrix} = \begin{bmatrix} 1 & \eta_e & 0 \\ 1 & \eta_{th} & \eta_H \end{bmatrix} \begin{bmatrix} P_e^{in} \\ P_g^{in} \\ P_h^{in} \end{bmatrix} \tag{2.1}$$

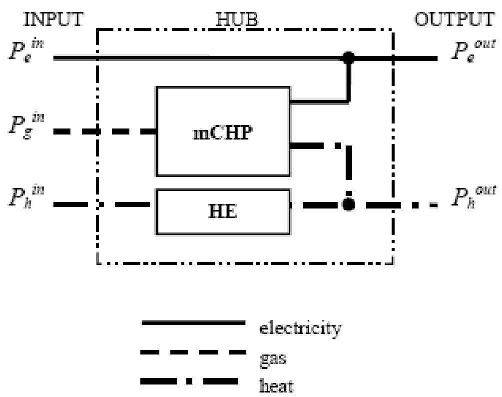


Figure 5: Energy hub model. The load connected to the output requires electricity and heat. Power conversion takes place in the µCHP and Heat Exchanger (HE) [6].

As given in [6], the cost function is defined as:

$$C_\alpha\left(P_\alpha^{in}\right) = a_{\alpha,0} + \begin{cases} \sum_{m=1}^{M_\alpha} a_{\alpha,m}\left(P_\alpha^{in}\right)^m & \text{for} \quad P_\alpha^{in} \geq 0 \\ \sum_{n=1}^{N_\alpha} b_{\alpha,n}\left(P_\alpha^{in}\right)^m & \text{for} \quad P_\alpha^{in} < 0 \end{cases} \tag{2.2}$$

The total energy cost for a customer is the sum of each energy costs:

$$C(\mathrm{P}^{in}) = \sum_{\alpha \in \varepsilon} C_\alpha \left(P_\alpha^{in}\right) \tag{2.3}$$

Where:

- $\varepsilon$ - Set of energy carriers taken into account
- C - Total cost of energy
- $C_\alpha$ - Individual costs according to (2.2)

The parameters of the energy cost function defined in equitation (2.2) are given in Table 2. The parameters describe the cost for energy carriers in the UK [7]. The variation of the cost functions with input power is shown in Figure 6.

Table 2: Coefficients for cost function (1) with $M_\alpha$= 2, $N_\alpha$= 1

| Energy carrier $\alpha$ | $a_{\alpha,0}$ [£] | $a_{\alpha,1}$ [£/kW] | $a_{\alpha,2}$ [£/kW$^2$] | $b_{\alpha,1}$ [£/kW] |
|---|---|---|---|---|
| electricity | 0.005 | 0.0957 | 0.001 | -0.07 |
| natural gas | 0.005 | 0.02856 | 0.001 | 0 |
| district heat | 0.005 | 0.0300 | 0.001 | 0 |

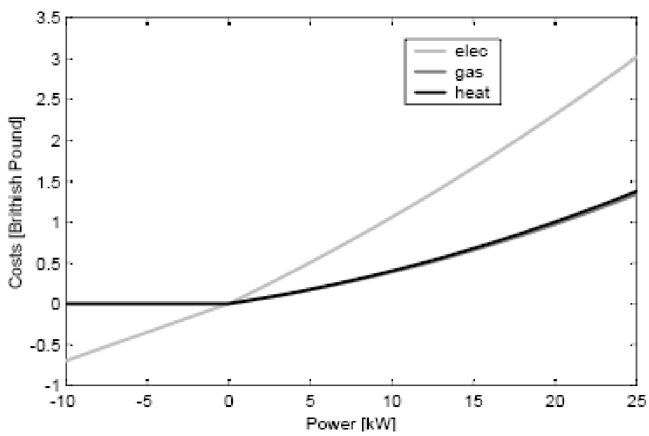


Figure 6: Cost functions for parameters described in Table 2

## 3.4 Control algorithms

In this section some of the control strategies used to control the μCHP installed in a hub are described.

(a) No μCHP in use [No μCHP]

This case is based on a hub without a μCHP unit. Therefore, there is no consumption of gas from the network, thus $P_g^{in}$ = 0. The reduced conversion equation is given by:

$$\begin{bmatrix} P_e^{in} \\ P_h^{in} \end{bmatrix} = \begin{bmatrix} 1 & 0 \\ 1 & \eta_H \end{bmatrix}^{-1} \begin{bmatrix} P_e^{out} \\ P_h^{out} \end{bmatrix} \qquad (2.4)$$

The power imported from the network was calculated by equation (2.4). Using the vector $\begin{bmatrix} P_e^{in} & P_h^{in} \end{bmatrix}^T$, the total cost of energy for a customer was calculated using cost functions (2.2) and (2.3).

(b) μCHP control based on cost optimisation [Cost optimisation]

This control algorithm was based on finding the optimal price of energy, minimising function (2.3), subject to constraints given in equation (2.1). In this case the optimisation algorithm with constraints was used [8], [9].

(c) μCHP control based on the heat demand [Heat demand]

In this case the μCHP was controlled to provide domestic heat demand locally. That is, there is no consumption of heat from the district heating network, thus $P_h^{in} = 0$. Then from equation (2.1), the electrical and gas imported to the hub was obtained as:

$$\begin{bmatrix} P_e^{in} \\ P_g^{in} \end{bmatrix} = \begin{bmatrix} 1 & \eta_e \\ 1 & \eta_{th} \end{bmatrix}^{-1} \begin{bmatrix} P_e^{out} \\ P_h^{out} \end{bmatrix} \tag{2.7}$$

Using the vector $\begin{bmatrix} P_e^{in} & P_g^{in} \end{bmatrix}^T$, the total cost of energy for a customer was calculated using cost functions (2.2) and (2.3).

(d) μCHP control based on electricity demand [Electricity demand]

In this case the μCHP is controlled to provide domestic electrical demand locally. That is, there is no consumption of electricity from the electrical power network, thus $P_e^{in} = 0$. Then from equation (2.1), the gas and heat imported to the hub was obtained as:

$$\begin{bmatrix} P_g^{in} \\ P_h^{in} \end{bmatrix} = \begin{bmatrix} \eta_e & 0 \\ \eta_{th} & \eta_H \end{bmatrix}^{-1} \begin{bmatrix} P_e^{out} \\ P_h^{out} \end{bmatrix} \tag{2.8}$$

Using the vector $\begin{bmatrix} P_g^{in} & P_h^{in} \end{bmatrix}^T$, the total cost of energy for a customer is calculated using cost functions (2.2) and (2.3).

(e) μCHP control based heuristic control [Combined]

This strategy is based on heuristic combination of the following control algorithms:

a. no μCHP control (a)
b. μCHP control based on the heat demand (c)
c. μCHP control based on the electricity demand (d)

The proposed algorithm was based on a simple cost optimisation of chosen controls. For a particular domestic demand, $P^{out}$ ($P_e^{out}$ and $P_h^{out}$), the power imported from the network, $P^{in}$ ($P_e^{in}$, $P_g^{in}$ and $P_h^{in}$) was calculated using equations (2.4), (2.7) and (2.8). Based on $P^{in}$ the total energy cost for each control strategy was calculated. Finally the cheapest control for the demand $P^{out}$ was chosen.

## 3.5 Case studies

The cost associated with different control strategies were obtained for different occupancy patterns for winter and summer. The data used for this study was based on reference [4]. Table 3 shows the occupancy patterns considered for the study.

Table 3: Occupancy patterns

| Occupancy pattern (OP) | Description | Unoccupied period |
|---|---|---|
| 1 | Part time work morning session | 9:00 to 13:00 |
| 2 | Full time work | 9:00 to 18:00 |
| 3 | Part time work | 9:00 to 16:00 |
| 4 | No work | N/A |

The winter and summer electricity and heat demands for different occupancy patterns considered in Table 3 are shown in Figure 7 and Figure 8 respectively.

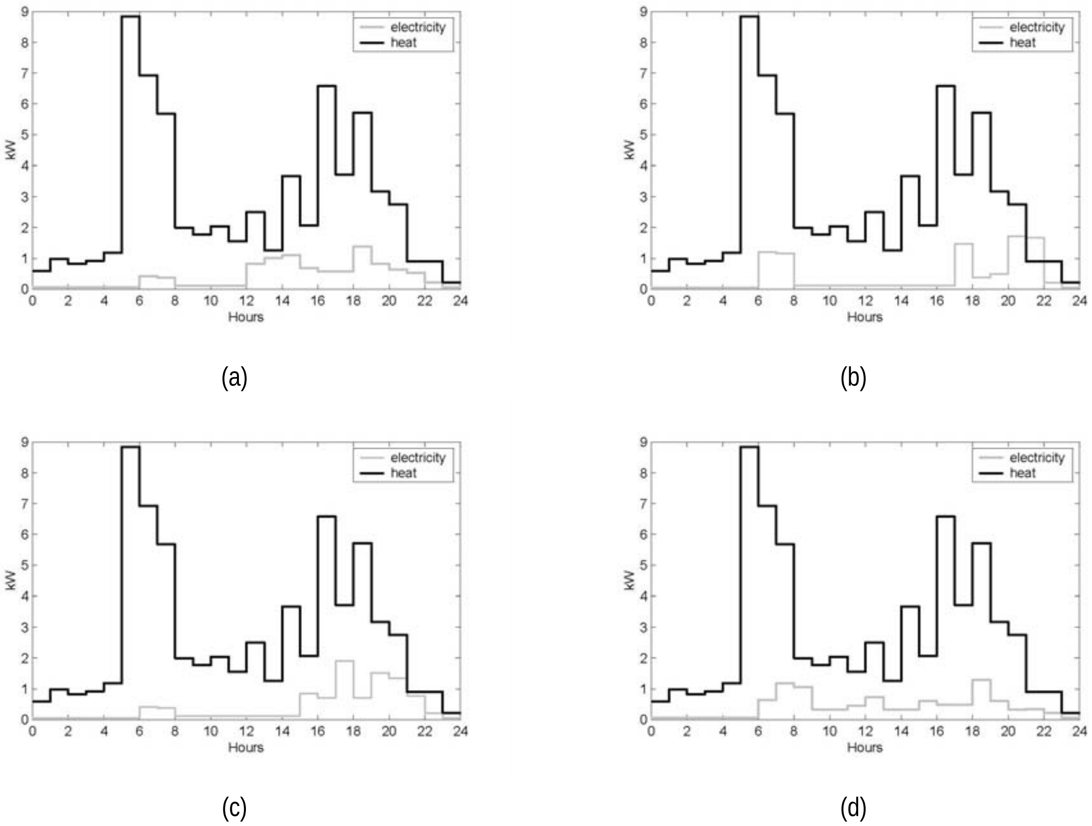


Figure 7: Winter demand, detached house, a) OP 1, b) OP 2, c) OP 3, and d) OP 4

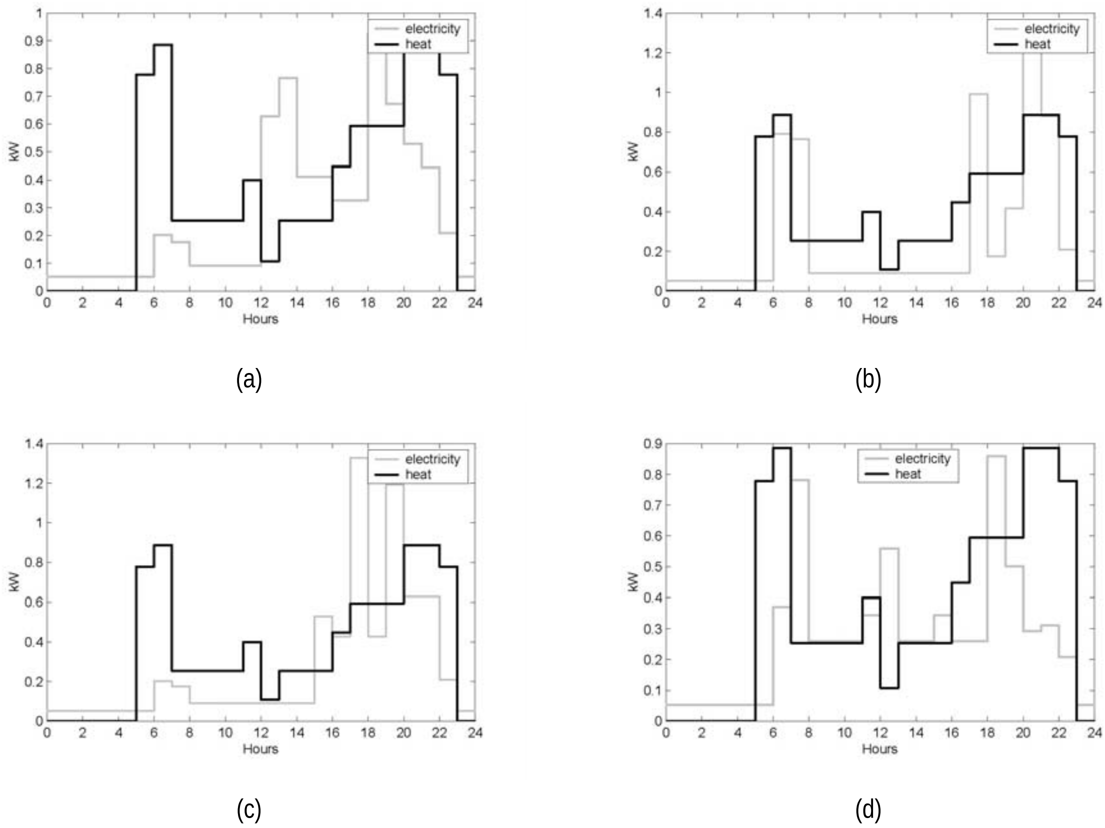

Figure 8: Summer demand, detached house, a) OP 1, b) OP 2, c) OP 3, and d) OP 4

## Control options for a μCHP under Combined control

For the combined control option given in 2.2(e), initially the cost associated with imported energy was calculated for each hour assuming either control options, ‘No μCHP’, ‘Heat Demand’ or ‘Electricity Demand’. The control option that gave the lowest cost was selected for that hour. Figure 9 shows the hourly selected control options for the μCHP unit for winter demand and Figure 10 shows this for summer demand.

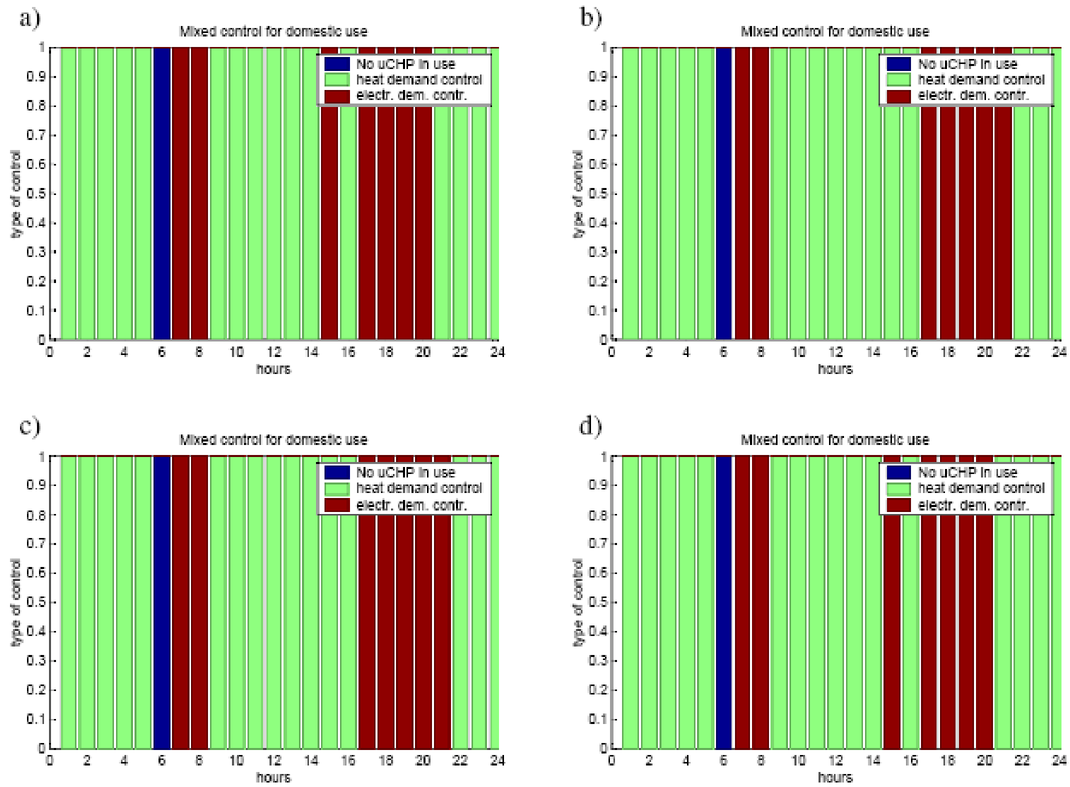


Figure 9: Hourly control of the µCHP for Winter demand, detached house, a) OP 1, b) OP 2, c) OP 3, and d) OP 4

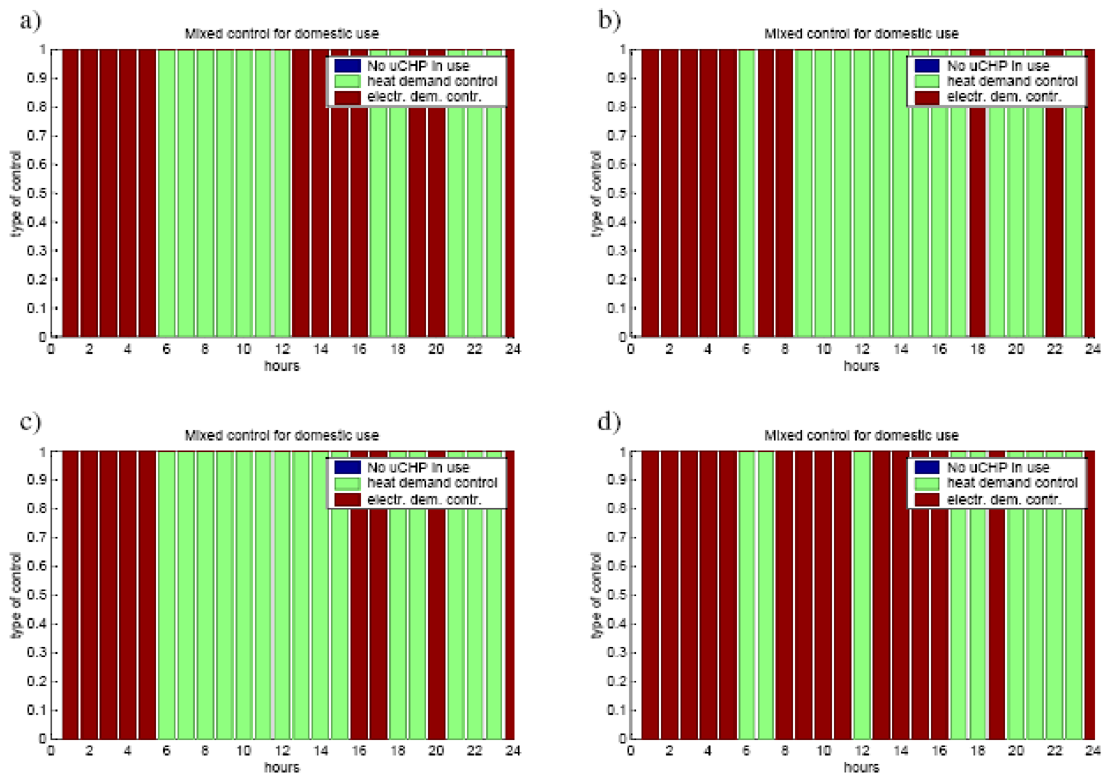


Figure 10: Hourly control of the µCHP for Summer demand, detached house, a) OP 1, b) OP 2, c) OP 3, and d) OP 4

Total cost for different control options

(a) Winter demand

Based on winter electricity and heat demands, the hourly and daily costs associated with a detached house was calculated for the five control options described in section 2.2. Table 4 presents the daily total cost of electricity, gas and heat for different occupancy patterns considered.

Table 5 shows the reduction of cost as a percentage with respect to the case where there is no µCHP (2.2(a)).

Table 4: Daily cost of imported energy for different control algorithms

| Control option as on section 2.2 | Daily cost of energy [£] | | | |
|---|---|---|---|---|
| | OP 1 | OP 2 | OP 3 | OP 4 |
| No µCHP | 3.64 | 3.61 | 3.64 | 3.65 |
| Cost optimisation | 2.88 | 2.88 | 2.88 | 2.89 |
| Heat demand | 3.68 | 3.68 | 3.68 | 3.69 |
| Electricity demand | 3.19 | 3.23 | 3.21 | 3.18 |
| Combined | 3.03 | 3.03 | 3.03 | 3.04 |

Table 5: Reduction of daily cost for different control algorithms

| Control option as on section 2.2 | Reduction of costs [%] | | | |
|---|---|---|---|---|
| | OP 1 | OP 2 | OP 3 | OP 4 |
| No µCHP | 0.00 | 0.00 | 0.00 | 0.00 |
| Cost optimisation | 20.94 | 20.30 | 20.98 | 20.95 |
| Heat demand | -1.17 | -1.96 | -1.09 | -1.07 |
| Electricity demand | 12.44 | 10.40 | 11.77 | 12.84 |
| Combined | 16.80 | 15.96 | 16.77 | 16.85 |

The hourly cost of electricity, gas and heat for occupancy patterns 2 and 3 are shown in Figure 11(a) and (b) respectively. Figure 12 and Figure 13 show the hourly change of energy imported form the network for different control options for occupancy patterns 2 and 3 respectively. Figure 14 and Figure 15 present the hourly change of energy produced by the µCHP (electricity, heat), and energy consumed by the µCHP (gas), for occupancy patterns 2 and 3 respectively.

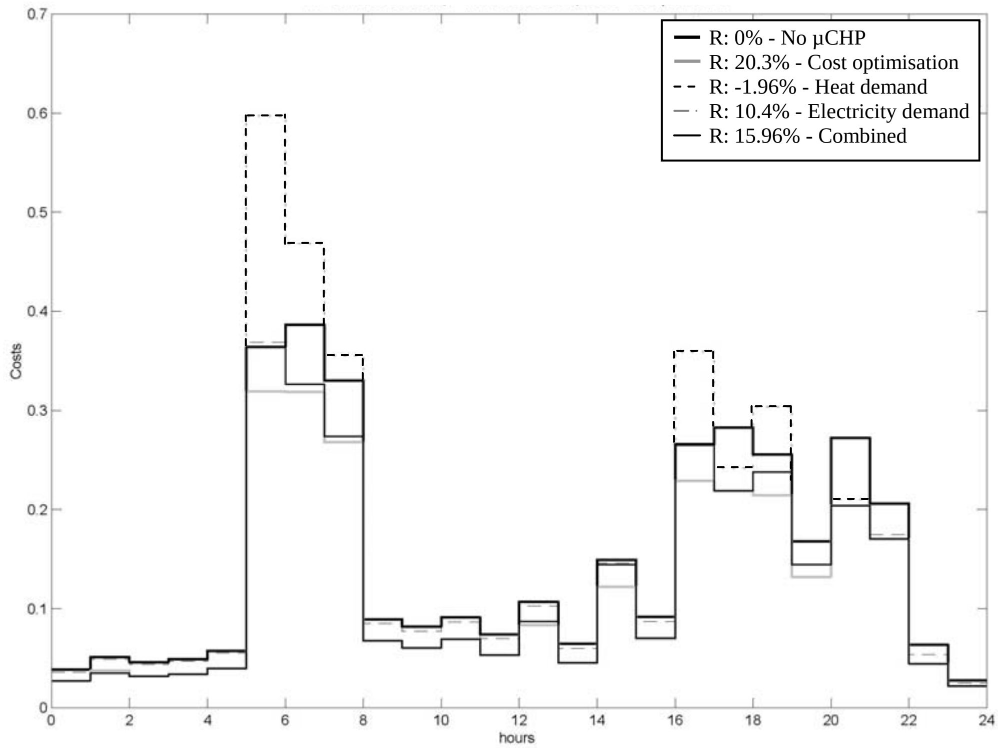


(a) For OP 2

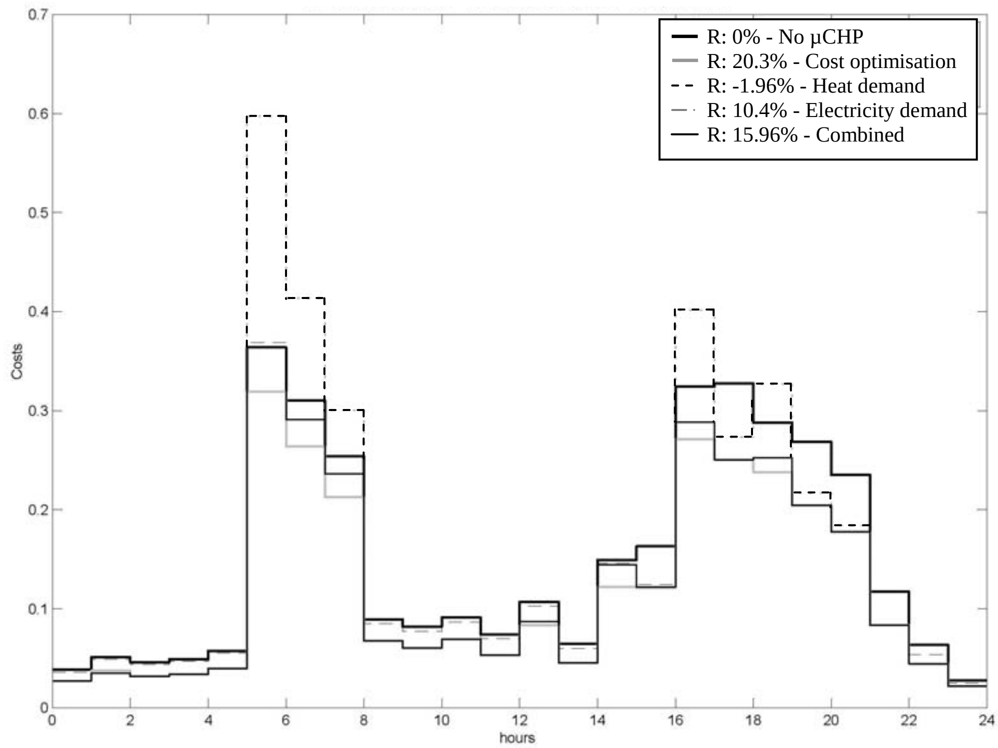


(a) For OP 3

Figure 11: Hourly costs for different control options

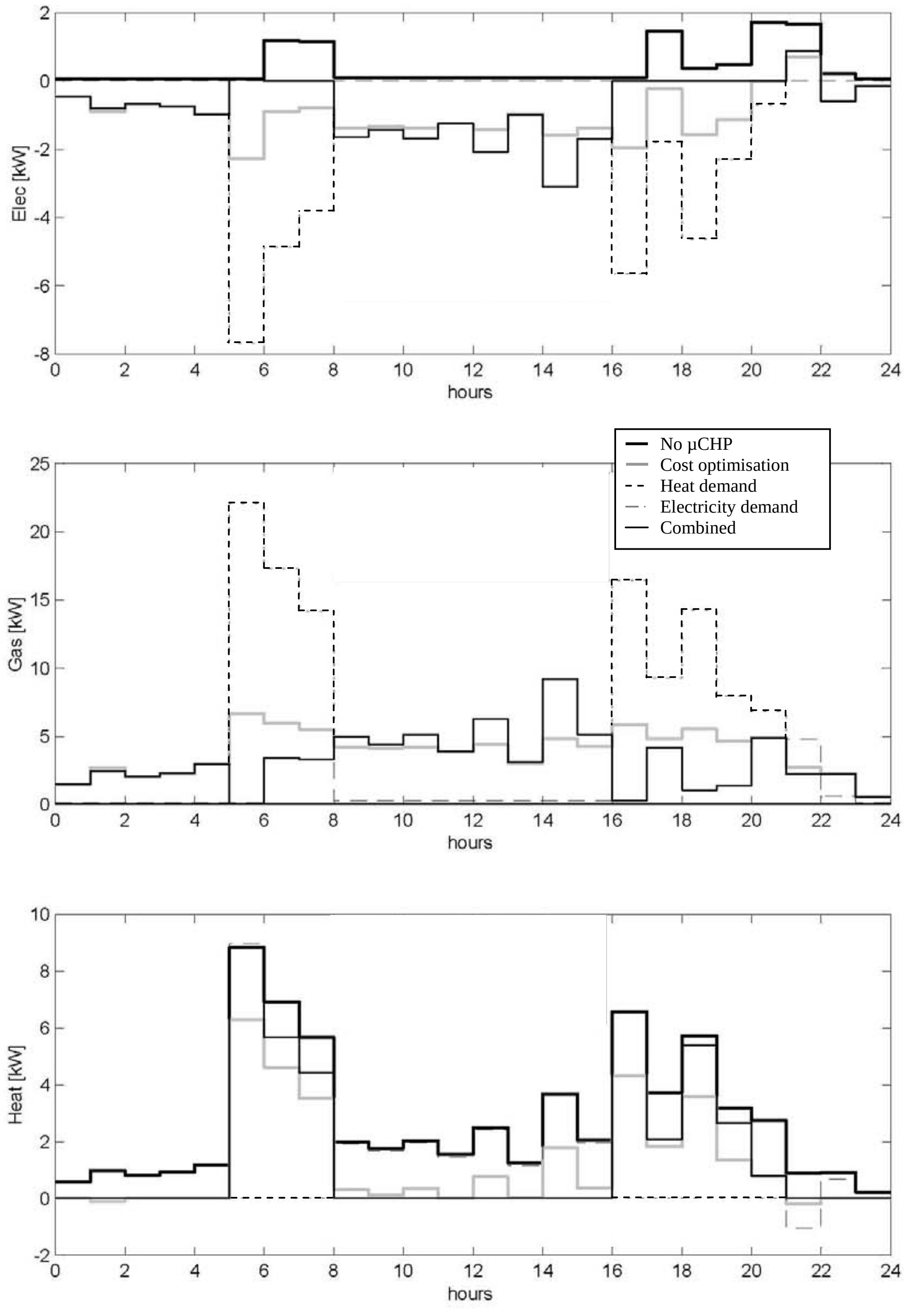


Figure 12: Hourly power imported from network for occupancy pattern 2

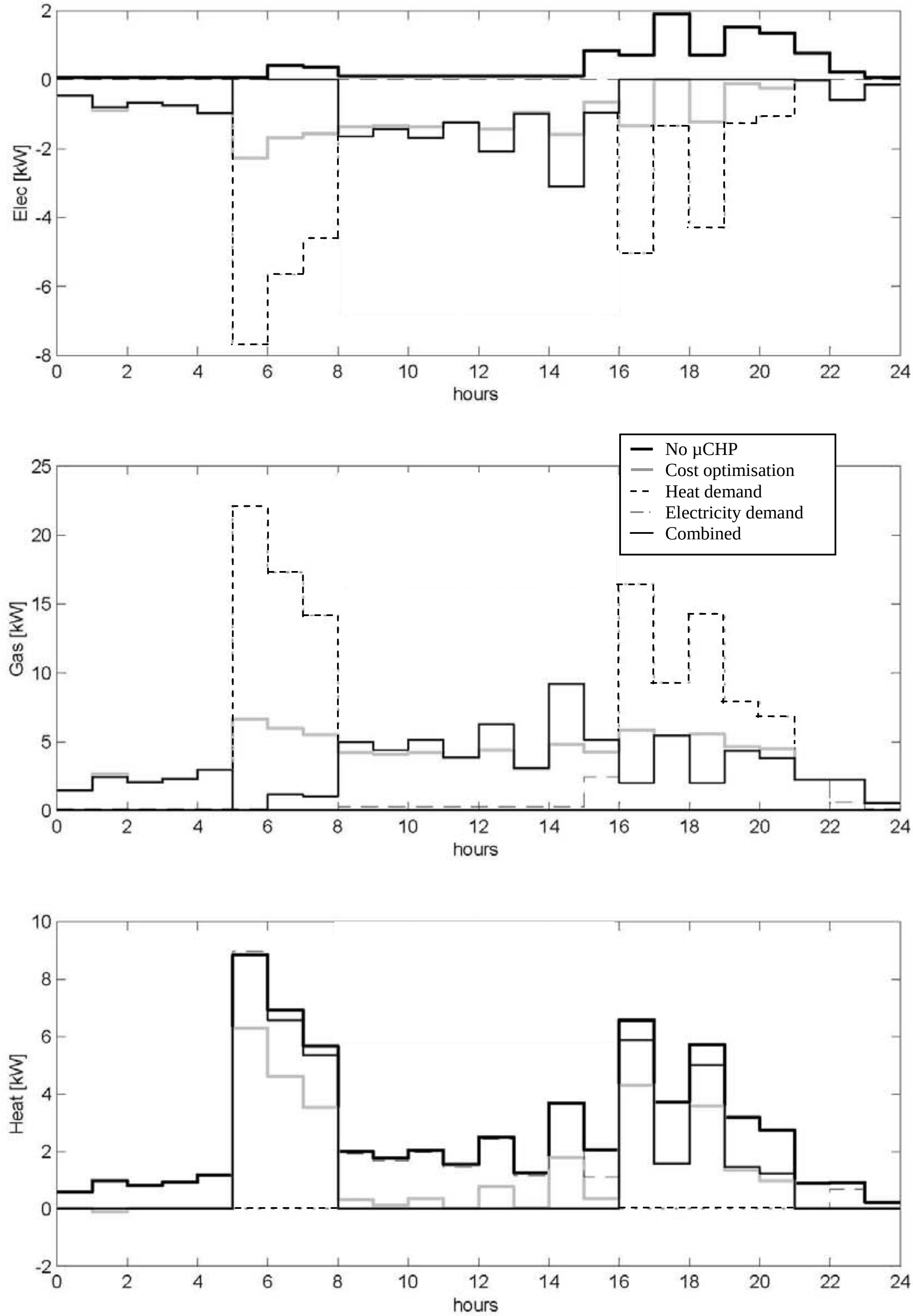


Figure 13: Hourly power imported from network for occupancy pattern 3

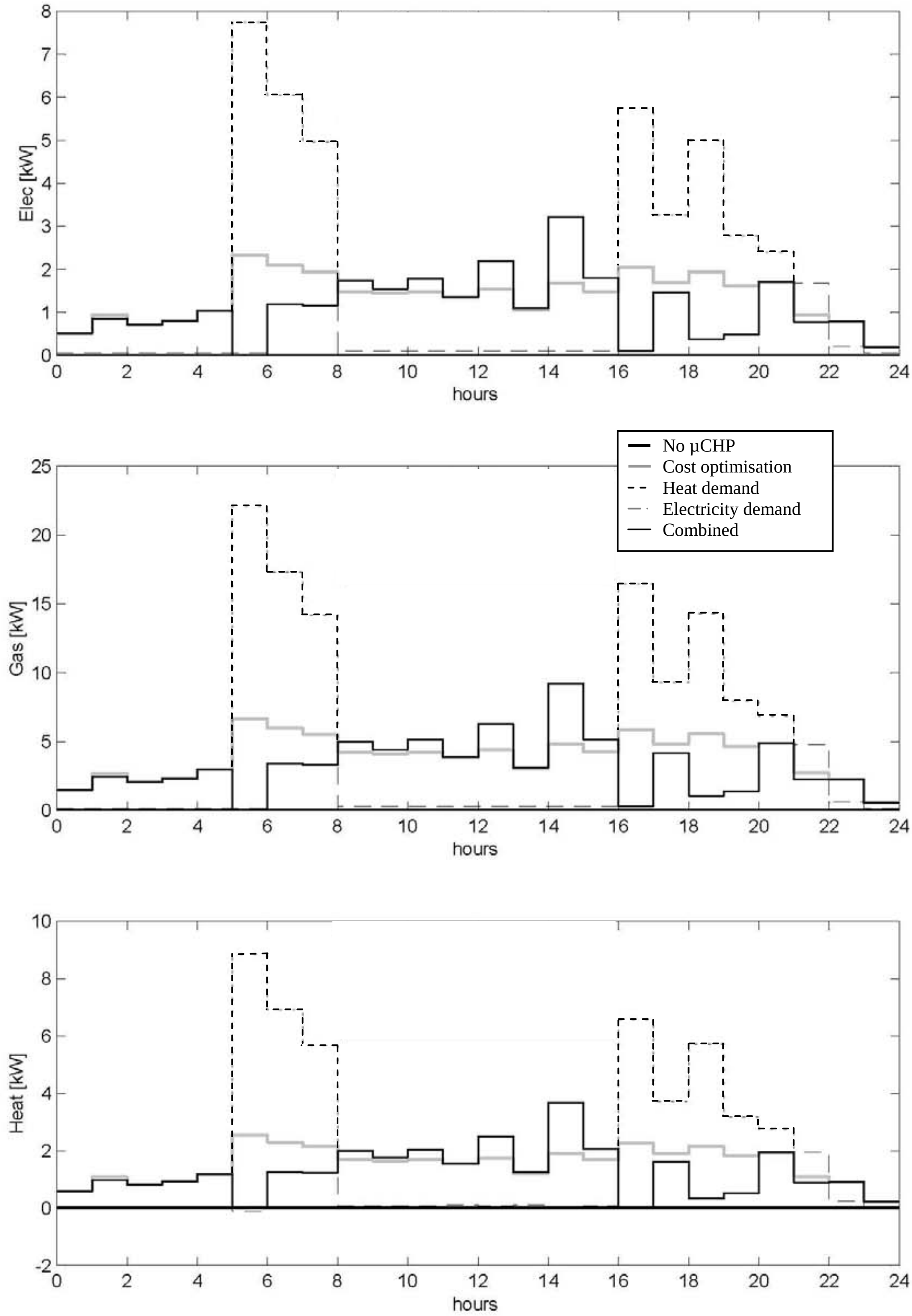


Figure 14: hourly changes of energy produced by µCHP (electricity, heat), and energy consumed by µCHP (gas) for occupancy pattern 2

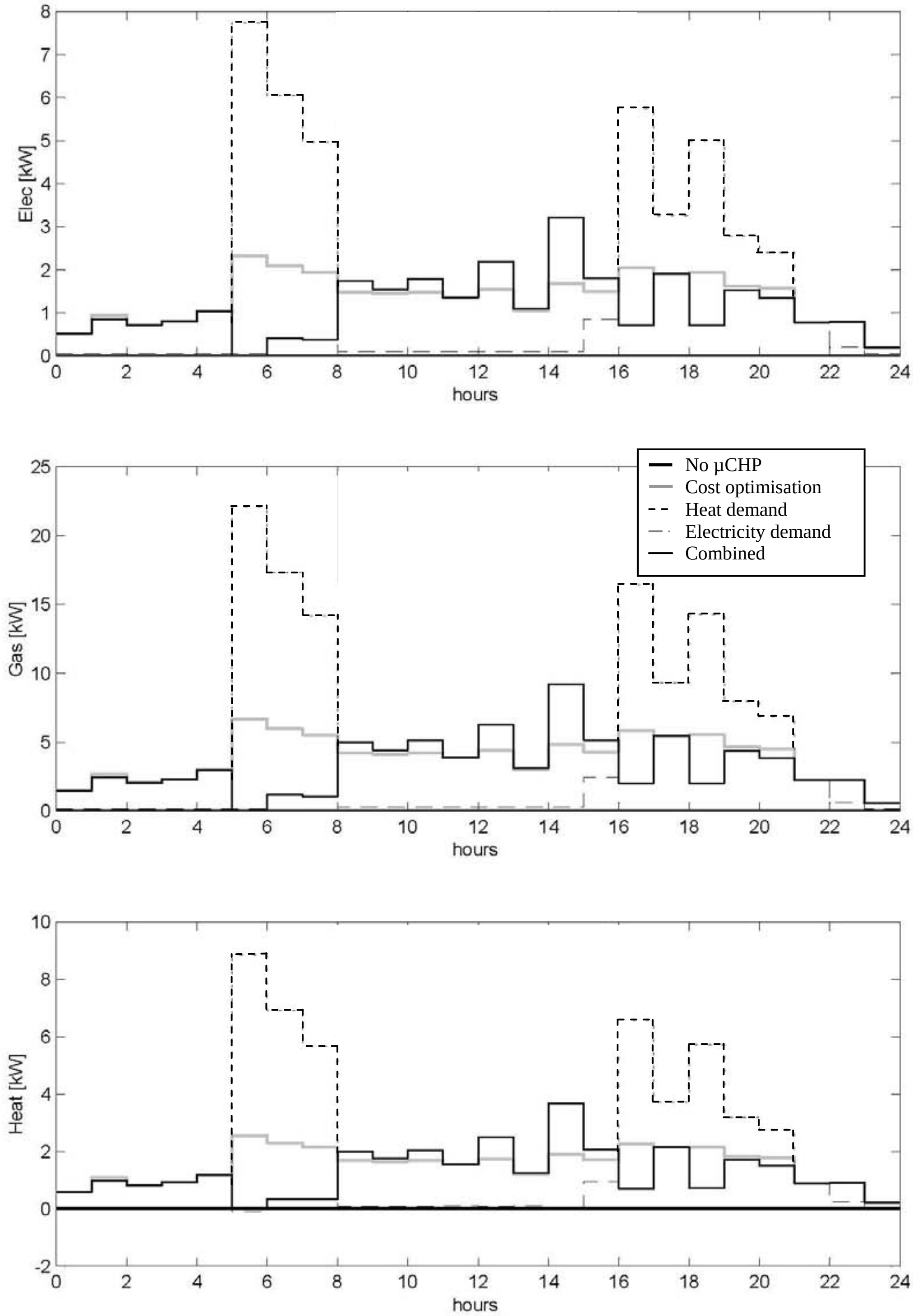


Figure 15: hourly changes of energy produced by µCHP (electricity, heat), and energy consumed by µCHP (gas) for occupancy pattern 3

(b) Summer demand

Based on summer electricity and heat demands, the hourly and daily costs associated with a detached house was calculated for the five control options described in section 2.2. Table 6 presents the daily total cost of electricity, gas and heat for different occupancy patterns considered. Table 7 shows the reduction of cost as a percentage with respect to the case where there is no µCHP (2.2(a)).

Table 6: Daily cost of imported energy for different control algorithms

| Control option as on section 2.2 | Daily cost of energy [£] | | | |
|---|---|---|---|---|
| | OP 1 | OP 2 | OP 3 | OP 4 |
| (a) | 1.28 | 1.28 | 1.28 | 1.28 |
| (b) | 1.00 | 1.00 | 1.00 | 0.99 |
| (c) | 1.02 | 1.01 | 1.01 | 1.01 |
| (d) | 1.05 | 1.06 | 1.06 | 1.04 |
| (e) | 1.00 | 1.00 | 1.00 | 0.99 |

Table 7: Reduction of daily cost for different control algorithms

| Control option as on section 2.2 | Reduction of costs [%] | | | |
|---|---|---|---|---|
| | OP 1 | OP 2 | OP 3 | OP 4 |
| (a) | 0.00 | 0.00 | 0.00 | 0.00 |
| (b) | 21.84 | 21.91 | 21.65 | 22.39 |
| (c) | 20.44 | 21.18 | 20.88 | 21.11 |
| (d) | 17.51 | 17.47 | 17.27 | 18.71 |
| (e) | 21.84 | 21.89 | 21.48 | 22.39 |

The hourly cost of electricity, gas and heat for occupancy patterns 2 and 3 are shown in Figure 16(a) and (b) respectively.

Figure 17 and Figure 18 show the hourly change of energy imported form the network for different control options for occupancy patterns 2 and 3 respectively. Figure 19 and Figure 20 present the hourly change of energy produced by the µCHP (electricity, heat), and energy consumed by the µCHP (gas), for occupancy patters 2 and 3 respectively.

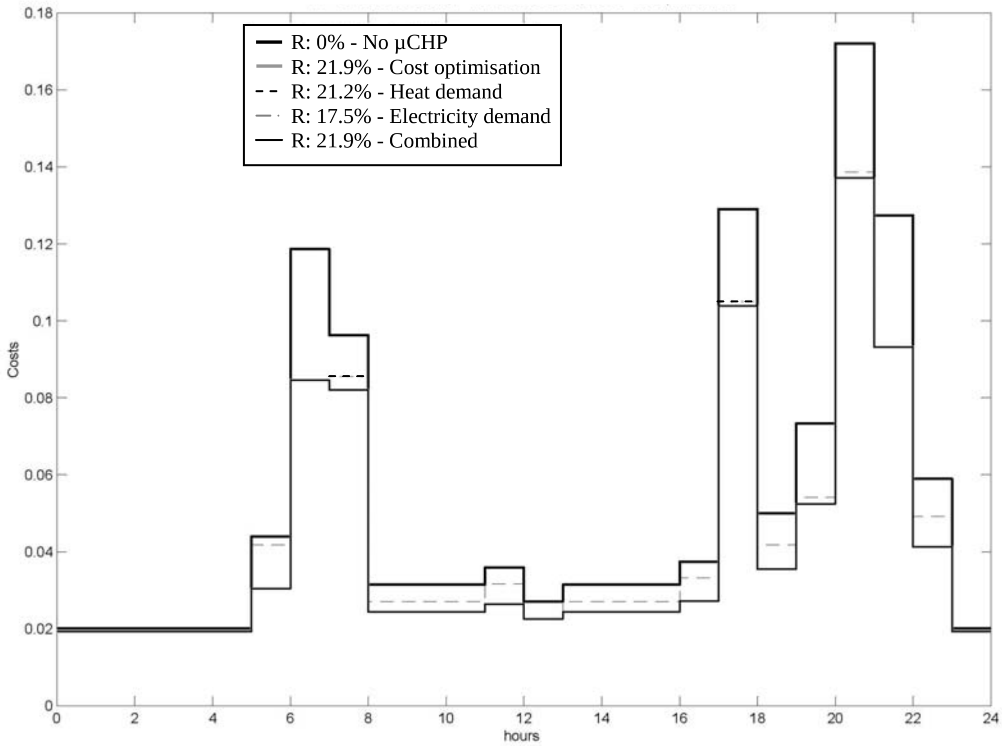


(a) For OP 2

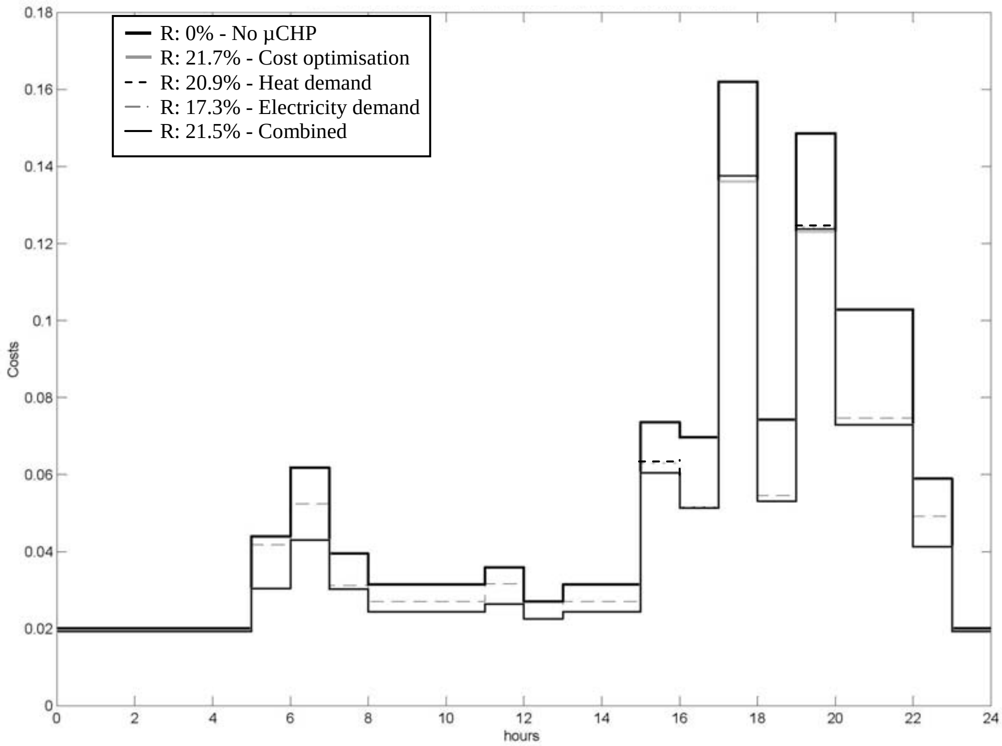


(a) For OP 3

Figure 16: Hourly costs for different control options

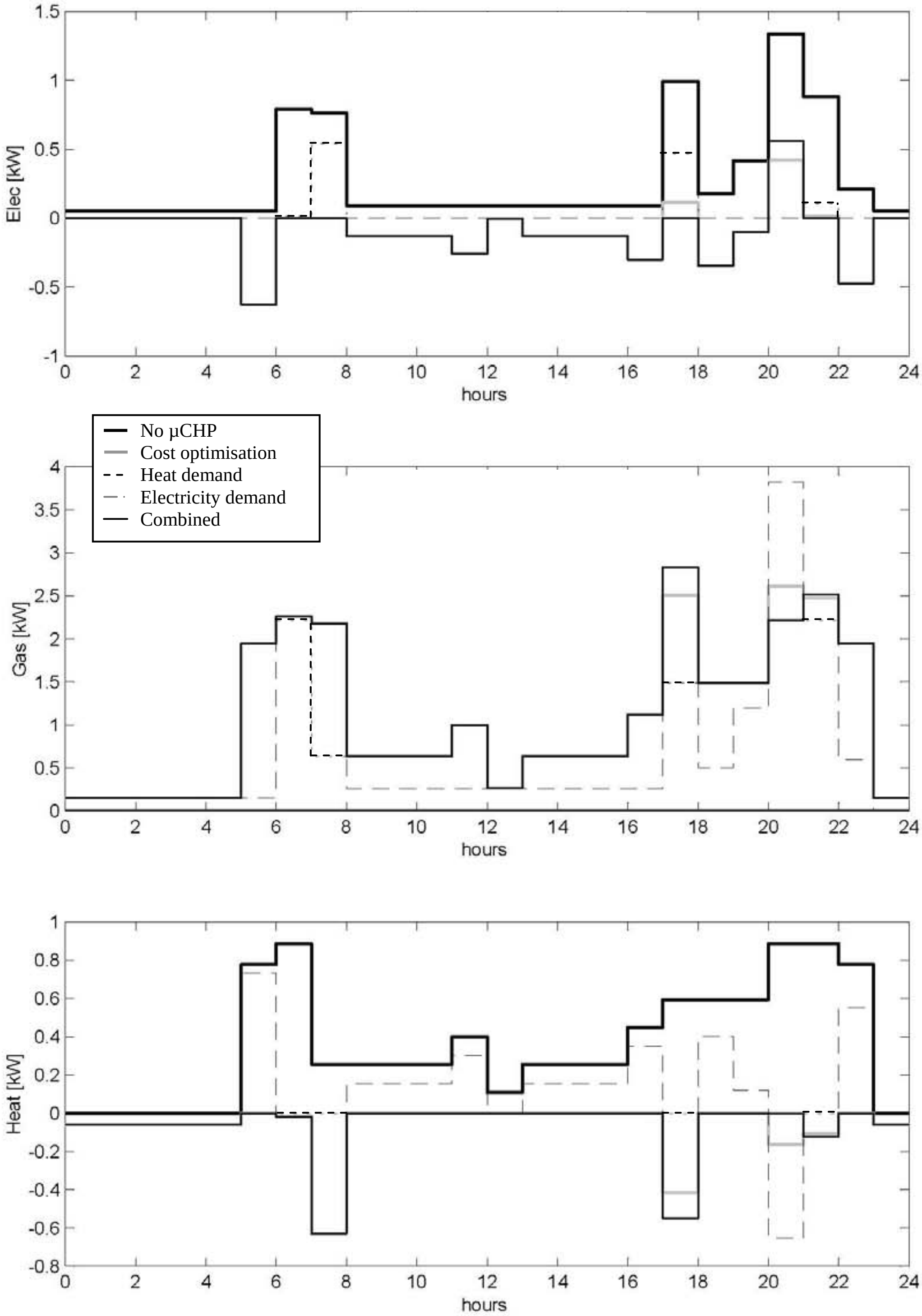


Figure 17: Hourly power imported from network for occupancy pattern 2

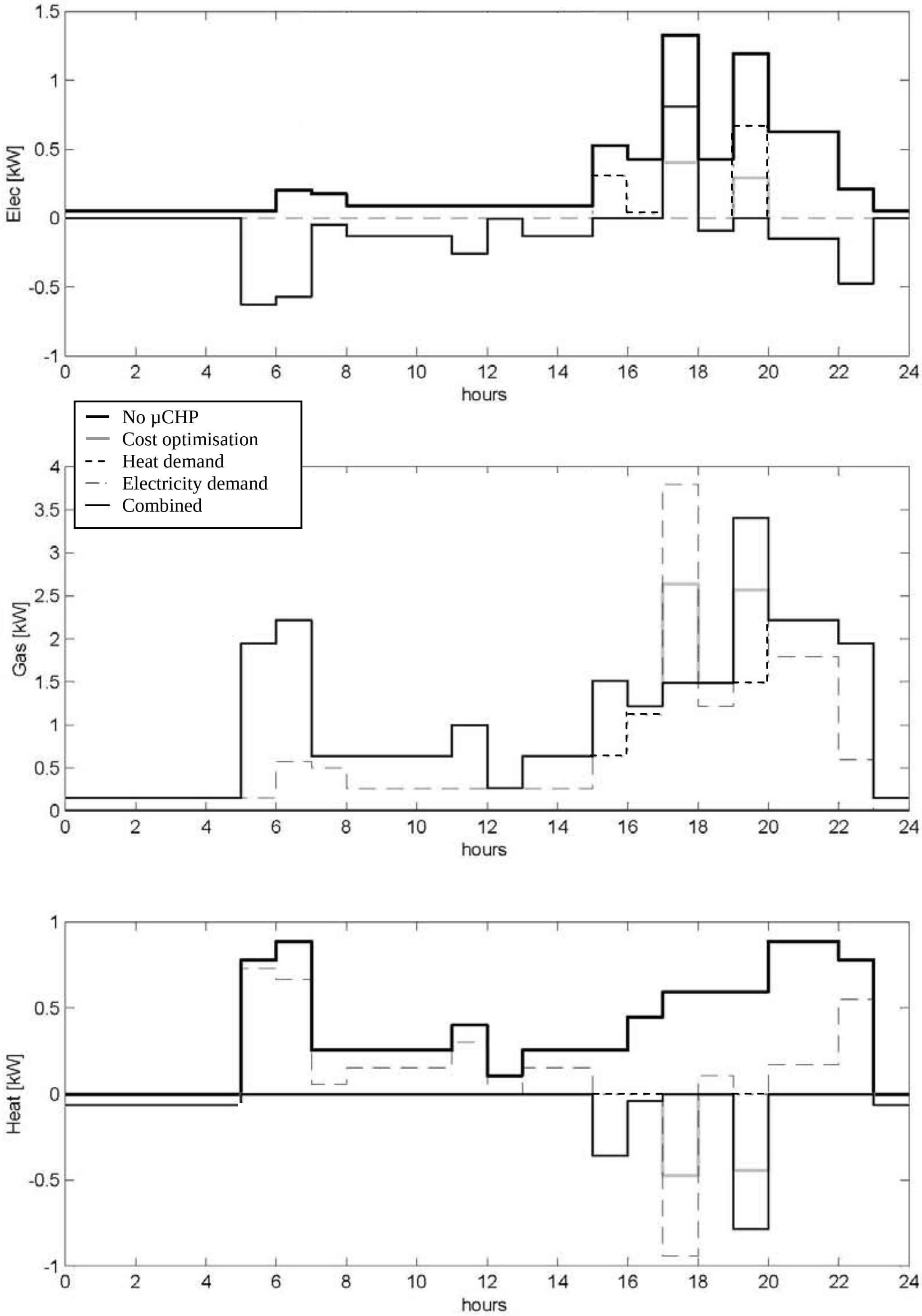


Figure 18: Hourly power imported from network for occupancy pattern 3

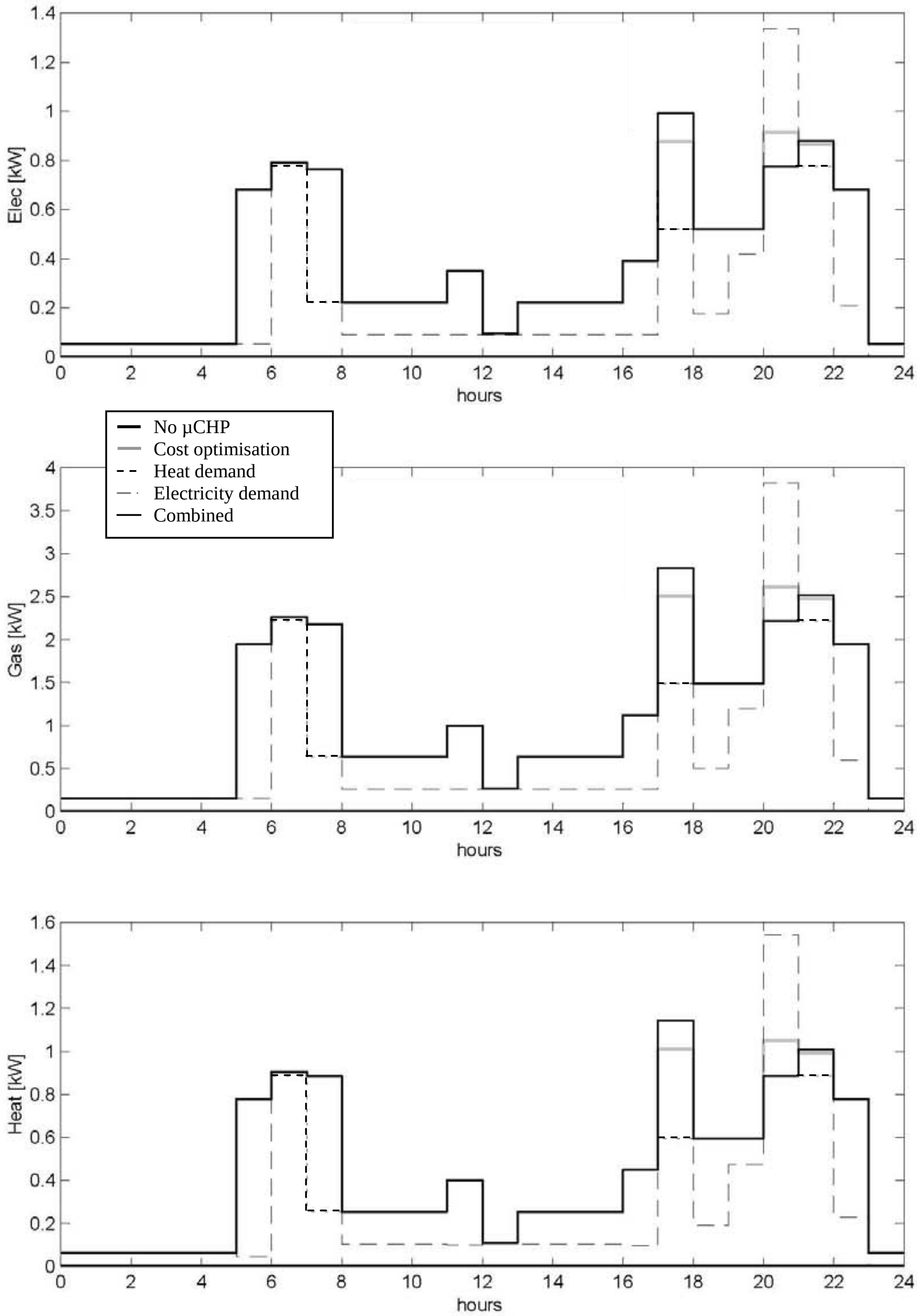


Figure 19: Hourly changes of energy produced by µCHP (electricity, heat), and energy consumed by µCHP (gas) for occupancy pattern 2

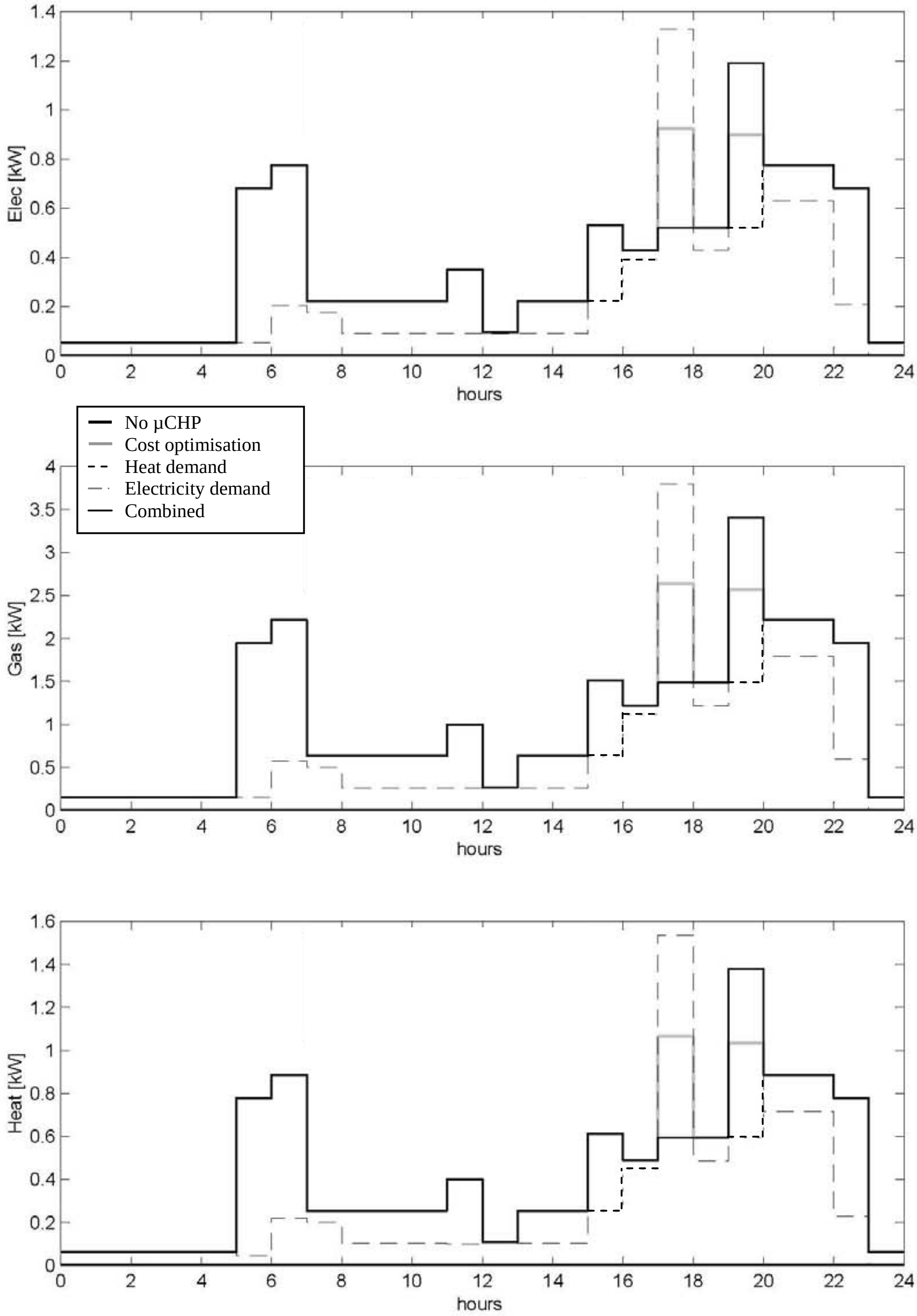


Figure 20: Hourly changes of energy produced by µCHP (electricity, heat), and energy consumed by µCHP (gas) for occupancy pattern 3

## 3.6 Discussion of results

The different control algorithms used to control a domestic µCHP unit was presented. The µCHP control based on cost optimisation provided the maximum benefits for an individual customer. For any occupancy pattern this method provided a cost reduction of more than 20% with respect to 'No µCHP' control (see Figure 21). This algorithm, despite the cost reduction, employs optimisation algorithms that cannot be cost-effectively implemented into a micro controller. Figure 21 clearly shows that other control strategies give a considerable cost reduction except in the case of 'Heat demand' control during the winter. In this case high heat demand compared to electricity demand, increases the cost of gas needed to produce heat. The control algorithm based on heuristic control shows comparable cost reduction with respect to that of cost optimisation.

The switching functions for the combined algorithm are presented in Figure 9 and Figure 10. It is possible to observe that for winter demand, the switching is not affected much by different occupancy patterns. For summer demand the switching functions are affected considerably by different occupancy patterns.

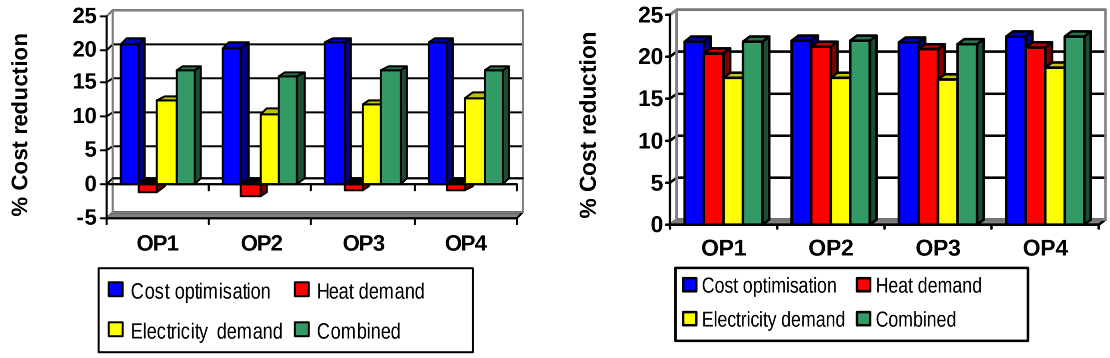


Figure 21: Daily reduction of cost for different control algorithms for a) winter demand, b) summer demand.

*Chapter 4*

# CONTROL ALGORITHMS FOR A ON-OFF TYPE µCHP UNIT

## 4.1 List of Symbols

| | |
|---|---|
| $f$ | Energy cost (pence) |
| $C_e$ | Electricity buy price (pence/kWh) |
| $C_s$ | Electricity sell price (pence/kWh) |
| $C_g$ | Unit cost of gas (pence/kWh) |
| $\Delta t$ | Time step used |
| $P_{demand}$ | Average electricity demand of the house within $\Delta t$ (kW) |
| $Q_{CHP}$ | Average gas consumption of the µCHP unit within $\Delta t$ (kW) |
| $P_{\mathrm{supply}}$ | Average grid electricity consumption within $\Delta t$ (kW) |
| $P_{losses}$ | Average electricity dumped or electricity sold within $\Delta t$ (kW) |
| $D_T$ | Average hot water demand within $\Delta t$ (kW) |
| $\eta_e$ | Electricity conversion efficiency of the µCHP unit |
| $\eta_{th}$ | Thermal conversion efficiency of the µCHP unit |
| $Q_{Boiler}$ | Average gas consumption of the boiler within $\Delta t$ (kW) |
| $\eta_b$ | Efficiency of the boiler |
| $CHP\_ON$ | ON time of the µCHP unit |

## 4.2 Introduction

In this chapter a µCHP unit that can operate on full-load and idling (or off) modes was considered. Two controlling modes of the µCHP are investigated. In the first controlling technique the µCHP was controlled to drive the space and hot water temperature towards two references without considering the cost of operation. This operation was then extended to minimise the cost of electricity and gas over a day.

## 4.3 Temperature driven control of the µCHP

(a) Control algorithm

The objective of the µCHP control is to drive the space and hot water temperature towards two predetermined reference settings ($\theta_{H,ref}$ and $\theta_{T,ref}$). These reference settings are normally set by the user based on the season and their occupancy pattern. The µCHP is controlled to drive $\theta_H(i+1)$ towards $\theta_{H,ref}$ and $\theta_T(i+1)$ towards $\theta_{T,ref}$.

Defining two constants, *D1* and *D2*, $\begin{bmatrix} D_1 \\ D_2 \end{bmatrix} = \begin{bmatrix} \mu_H & 0 \\ L_T\alpha_T & \mu_T \end{bmatrix} \begin{bmatrix} \theta_H(i) \\ \theta_T(i) \end{bmatrix} + \begin{bmatrix} L_H\alpha_H\theta_A \\ -\alpha_T D_T \end{bmatrix}$, equation (1.5) was re-written as:

$$\begin{bmatrix} \theta_H(i+1) \\ \theta_T(i+1) \end{bmatrix} = \begin{bmatrix} \alpha_H & 0 \\ 0 & \alpha_T \end{bmatrix} \begin{bmatrix} Q_H \\ Q_T \end{bmatrix} + \begin{bmatrix} D_1 \\ D_2 \end{bmatrix} \quad (4.1)$$

When the µCHP is ON, it produces a constant heat output of $Q_C$ and thus $Q_H + Q_T = Q_C$. By substituting for $Q_T = Q_C - Q_H$ into equations (4.1), the following two equations were obtained:

$$\begin{aligned} \theta_H(i+1) - \alpha_H Q_H &= D_1 \\ \theta_T(i+1) + \alpha_T Q_H &= D_2 + \alpha_T Q_C \end{aligned} \quad (4.2)$$

By eliminating $Q_H$ from equation (4.2), the following equation was obtained:

$$\alpha_T\theta_H(i+1) + \alpha_H\theta_T(i+1) = \alpha_T D_1 + \alpha_H D_2 + \alpha_H\alpha_T Q_C \quad (4.3)$$

In order to drive the space and hot water temperature towards their respective references, the control function defined in Figure 22 was used. In this figure, $\varepsilon_H$ and $\varepsilon_T$ are the allowable tolerances for space and hot water temperature.

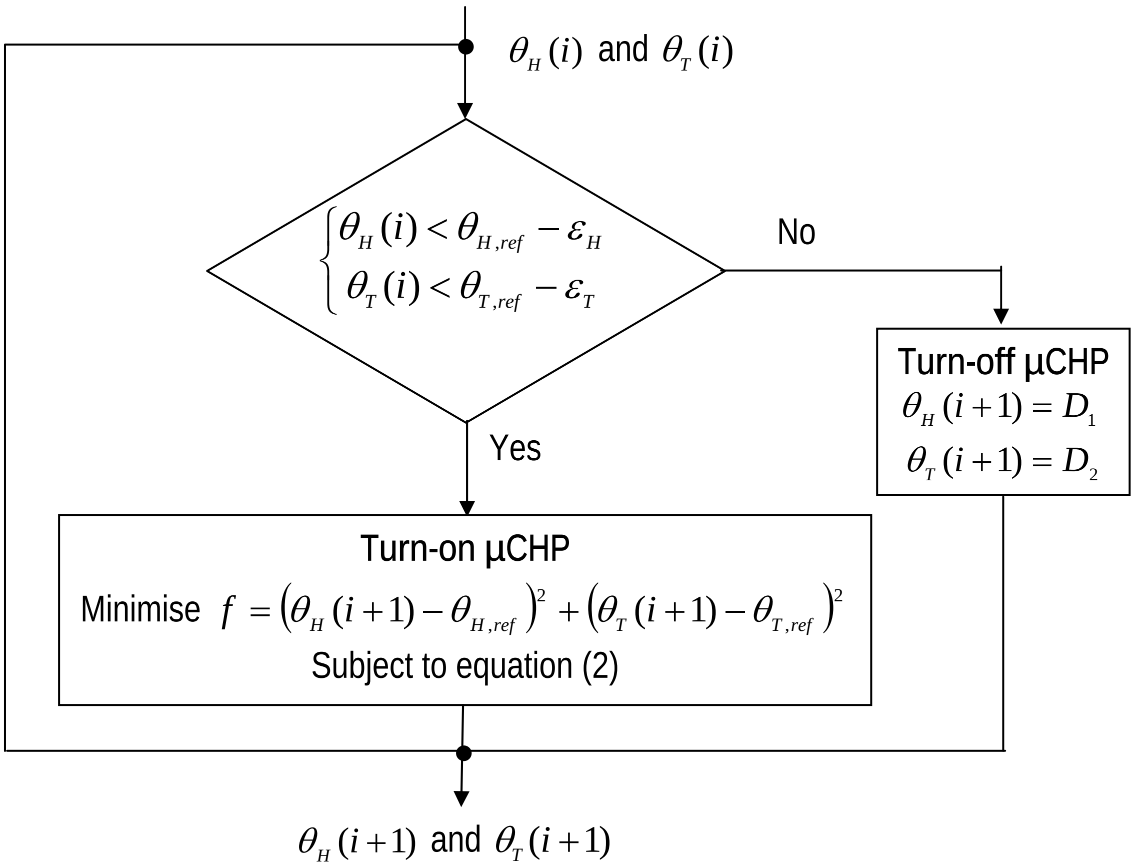


Figure 22: Algorithm used for temperature control

### (b) Case study

A 7 kW µCHP unit with thermal conversion efficiency of 80% and electrical conversion efficiency of 10% was considered for this study.

The data used for the simulations are given in Appendix A [5]. Figure A1 shows the seasonal and weakly electricity load profiles. Figure A2 shows the hot water demand profiles, which were calculated based on the following procedure:

(a) Based on the hot water demand (in litres) profiles given in reference [5], the average temperature of the water inside the hot water tank was estimated. It was assumed that once the hot water is used, cold water will be pumped into the tank.

(b) Then the heat required to raise the temperature of the water inside the tank to 50°C was estimated.

(c) The average power required was estimated based on the heat demand.

Typical outside temperature profiles for different seasons are shown in Figure A3.

The house with the µCHP unit was modelled using equation (4.1) and control algorithm defined in Figure 22. Figure 23 shows the response of the temperature controller for a typical winter day.

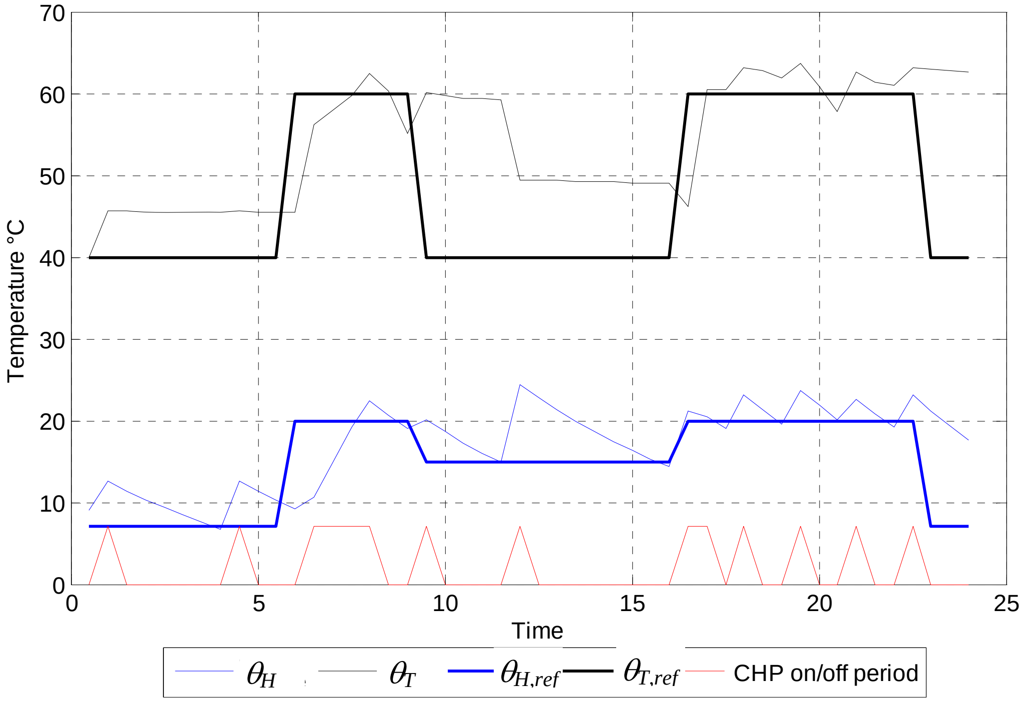


Figure 23: House and hot water temperature from simplified and full models

## 4.4 Optimum cost control of the µCHP

### (a) Total cost of gas and electricity for a single dwelling

Total cost of gas and electricity for a house with the µCHP unit was considered for the following two cases:

i) No provision for selling electricity from the µCHP

When demand is greater than generation

$$C_{total} = C_g Q_{CHP} \Delta t + C_e (P_{demand} - \eta_e Q_{CHP}) \Delta t \qquad (4.4)$$

When demand is less than generation

$$C_{total} = C_g Q_{CHP} \Delta t \tag{4.5}$$

ii) With provision for selling electricity from the µCHP

When demand is greater than generation

$$C_{total} = C_g Q_{CHP} \Delta t + C_e (P_{demand} - \eta_e Q_{CHP}) \Delta t \tag{4.6}$$

When demand is less than generation

$$C_{total} = C_g Q_{CHP} \Delta t - C_s (\eta_e Q_{CHP} - P_{demand}) \Delta t \tag{4.7}$$

(b) Optimum cost operation of the $\mu$CHP

The purpose of this control is to minimise the total cost of gas and electricity ( $f$ ) whilst maintaining the temperature inside the house and hot water tank within the required bounds. The problem was formulated in an optimisation package with a time step of 0.5 hrs.

When there is no provision for selling electricity, the objective is to minimise the costs associated with gas utilised for the operation the µCHP unit and electricity costs due to electrical demand that is not met by the µCHP unit. From equations 4.4 and 4.5:

$$\text{Minimise } f = \sum_{t=0}^{t=23.30} 0.5 \times \left[ C_g Q_{CHP}(t) + C_e(t) \times P_{\text{supply}}(t) \right] \tag{4.8}$$

When there is provision for selling electricity, the objective function is supplemented with the option to sell electricity to the grid. From equations 4.6 and 4.7:

$$\text{Minimise } f = \sum_{t=0}^{t=23.30} 0.5 \times \left[ C_g Q_{CHP}(t) + C_e(t) \times P_{\text{supply}}(t) + C_s(t) \times P_{\text{losses}}(t) \right] \tag{4.9}$$

Subject to:

1. Electrical energy balance constraints

$$P_{\text{supply}}(t) + \eta_e Q_{CHP}(t) = P_{demand}(t) + P_{losses}(t)$$

2. Heat constraints

$$\begin{bmatrix}\theta_H(t)\\ \theta_T(t)\end{bmatrix}=\begin{bmatrix}\mu_H & 0\\ L_T\alpha_T & \mu_T\end{bmatrix}\begin{bmatrix}\theta_H(t-0.5)\\ \theta_T(t-0.5)\end{bmatrix}+\begin{bmatrix}\alpha_H & 0\\ 0 & \alpha_T\end{bmatrix}\begin{bmatrix}Q_H(t-0.5)\\ Q_T(t-0.5)\end{bmatrix}+\begin{bmatrix}L_H\alpha_H\theta_A(t-0.5)\\ -\alpha_T D_T(t-0.5)\end{bmatrix}$$

$$Q_H(t)+Q_T(t)=\eta_{th}Q_{CHP}(t)$$

Bounds:

1. Temperature constraints

$$\begin{bmatrix}\theta_{H,ref,\min}\\ \theta_{T,ref,\min}\end{bmatrix}\le\begin{bmatrix}\theta_H(t)\\ \theta_T(t)\end{bmatrix}<\begin{bmatrix}\theta_{H,ref,\max}\\ \theta_{T,ref,\max}\end{bmatrix}$$

The minimum and maximum bounds for space and hot water temperatures were defined to represent seasonal variations and the comfort of residents.

2. Capacity constraints

$$Q_{CHP}(t)=\begin{cases}7\text{ kW when uCHP is ON}\\ 0\quad\text{when uCHP is OFF}\end{cases}$$

## 4.5 Case studies

A number of case studies were carried out to demonstrate the benefits of the optimum cost control strategy of the µCHP against a temperature controlled scheme. The reference settings for space and hot water temperatures were defined for a typical weekday, Saturday and Sunday for winter, summer and autumn/spring. Half hourly data was used as electricity in the UK is traded in half hourly windows.

It was assumed that the electricity buy price, $C_e$, varies with time (follows the demand curve) with an average price of 10 pence/kWh (see Figure A4). Even though the domestic cost of electricity is based on a constant tariff, a varying cost function was assumed in order to represent the avoided generation cost of electricity due to locally produced electricity by the µCHP unit. The selling price of electricity was assumed as being two pence lower than the buying price.

Using the daily profiles given in Appendix A and employing the linear programming optimisation routine from the Dash Xpress optimisation suite [10], the optimum cost of gas and electricity for the µCHP control was calculated. Figure 24 shows the total cost of gas and electricity over a day, when the µCHP is on temperature controlled mode (TC) and when it is on optimum cost controlled mode (OC). Figure 24(a) shows the comparison for a typical weekday, Saturday and Sunday in winter. Figure 24(b) and (c) shows similar results for autumn/spring and summer.

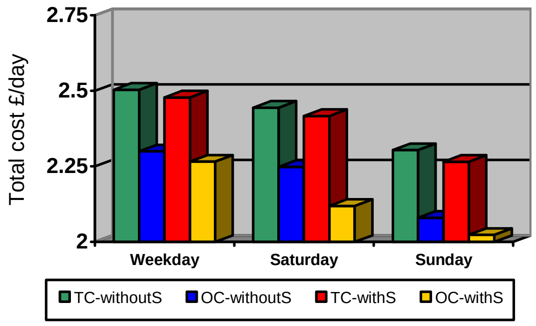


(a) Total gas and electricity cost for a typical winter day

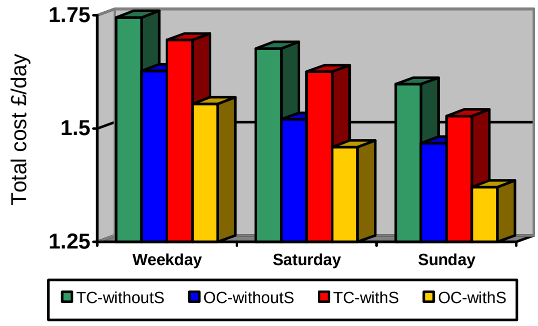


(b) Total gas and electricity cost for a typical Autumn/spring day

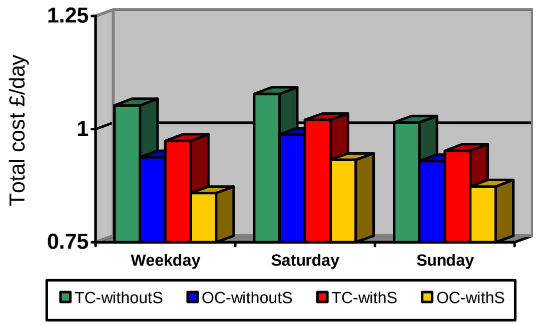


(c) Total gas and electricity cost for a typical summer day

Figure 24: Cost saving with temperature controlled (TC) and optimum cost control (OC) strategies; withoutS – no provision for selling electricity; withS - with provision for selling electricity

Figure 25 shows the temperature profiles that are obtained from the temperature controlled and optimum cost controlled strategies with turn-on and turn-off times of the µCHP unit for a winter weekday, Saturday and Sunday. Both modes of control were used to maintain the temperature inside the house and hot water temperature within the required bounds. The lower reference bounds are also shown in Figure 25, which were determined to reflect typical occupancy patterns during week days and weekends.

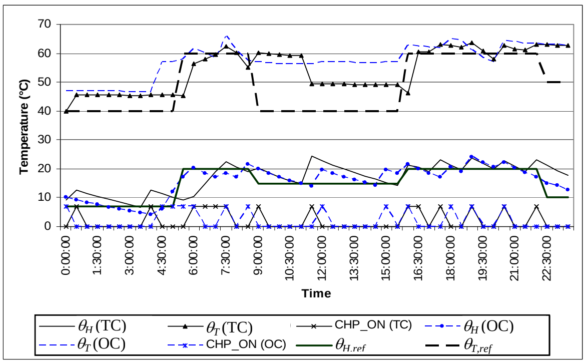


(a) For a winter weekday

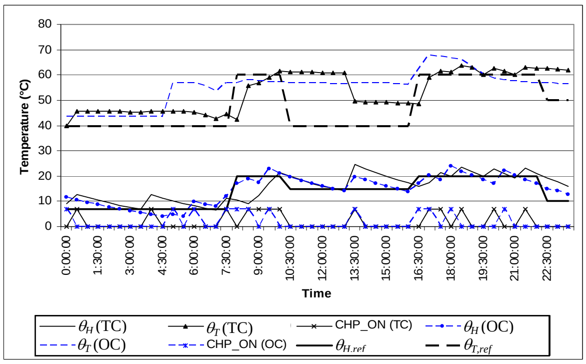


(b) For a winter Saturday

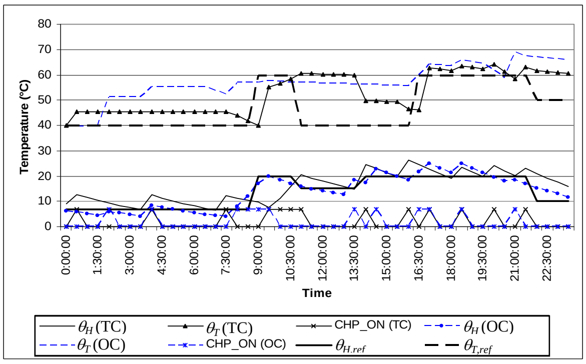


(c) For a winter Sunday

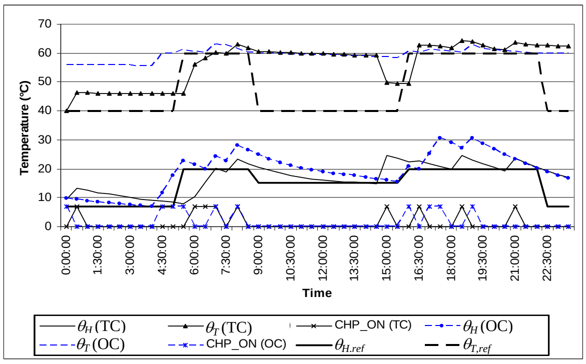


(d) For a spring/autumn weekday

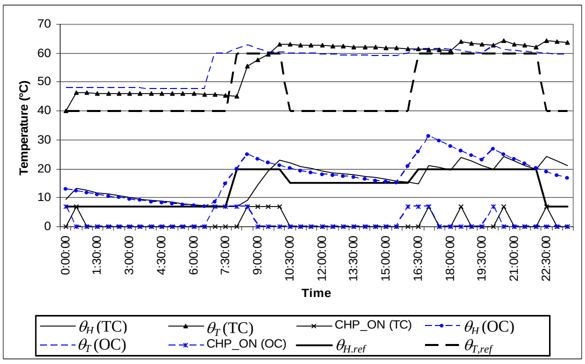


(e) For a spring/autumn Saturday

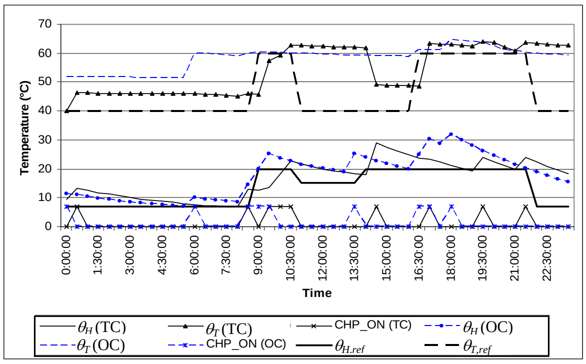


(f) For a spring/autumn Sunday

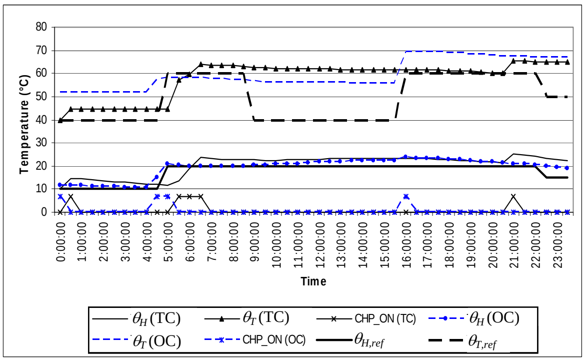


(g) For a summer weekday

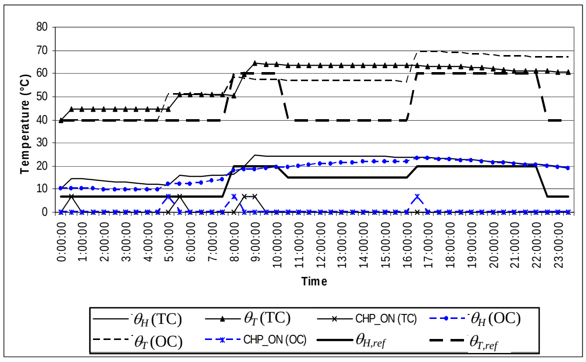


(h) For a summer Saturday

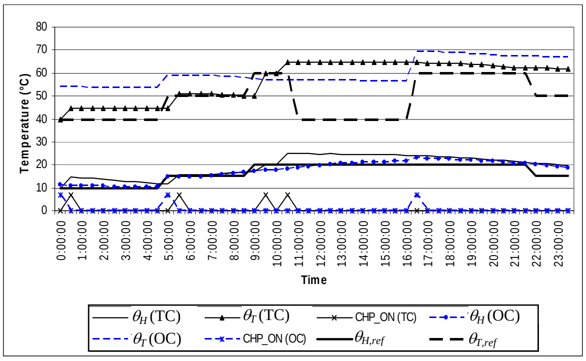


(i) For a summer Sunday

Figure 25: Temperature profile for temperature controlled (TC) and optimum cost control (OC) strategies with no provision for selling electricity

## 4.6 Results

Table 8 summarises the total cost of gas and electricity for different control strategies.

Table 8: Summery of the results

| Type | Cost without selling electricity (£/year) | Cost with selling electricity (£/year) |
|---|---|---|
| Conventional boiler [3] | 844.62 | - |
| The µCHP on continuous output mode [3] | 803.85 | 608.56 |
| The µCHP on ON-OFF mode and on temperature controlled mode | 634.68 | 615.83 |
| The µCHP on ON-OFF mode and on optimum cost controlled mode | 583.24 | 559.42 |

## 4.7 Modelling two semi-detached houses

(a) Optimum cost operation of the $\mu$CHP unit and Boiler

Two semi-detached houses shown in Figure 26, were modelled for this study. The electrical and thermal networks for the two semi-detached houses were considered to be interconnected. One house had a 7 kW µCHP unit and the other a 10 kW Boiler.

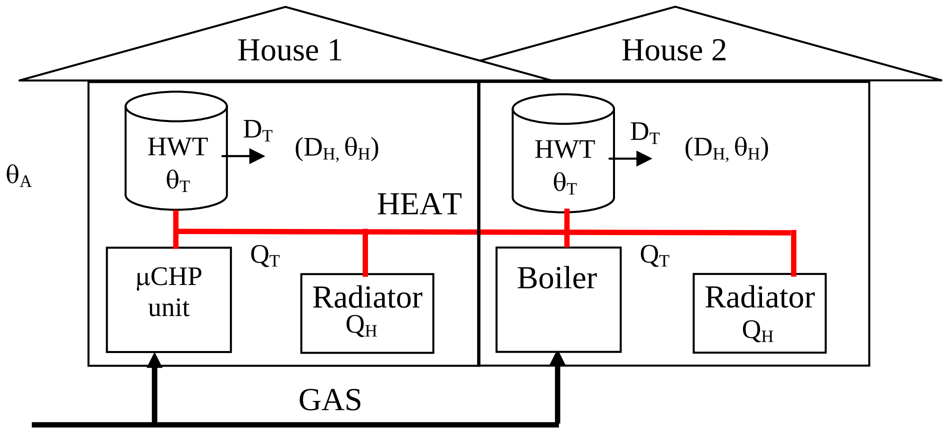


Figure 26: Two-house model

The following is assumed:

1. The µCHP and the boiler were controlled to supply heat for both houses.
2. The electricity produced by the µCHP is also supplied to both houses.
3. The heat loss in the pipes is negligible and the two houses have identical thermal properties.

In order to optimise the cost of gas and electricity the following procedure was used.

Minimise $f = \sum_{t=0}^{t=23.30} 0.5 \times \left[ C_g Q_{CHP}(t) + C_g Q_{Boiler}(t) + C_e(t) \times P_{\text{supply}}(t) \right]$

Subject to (subscript 1 stands for 1st house and 2 stands for 2nd house):

1. Electrical energy balance constraints

$$P_{\text{supply}}(t) + \eta_e Q_{CHP}(t) = P_{demand1}(t) + P_{demand2}(t) + P_{losses}(t)$$

2. Heat constraints

$$\begin{bmatrix} \theta_{H1}(t) \\ \theta_{T1}(t) \end{bmatrix} = \begin{bmatrix} \mu_H & 0 \\ L_T\alpha_T & \mu_T \end{bmatrix} \begin{bmatrix} \theta_{H1}(t-0.5) \\ \theta_{T1}(t-0.5) \end{bmatrix} + \begin{bmatrix} \alpha_H & 0 \\ 0 & \alpha_T \end{bmatrix} \begin{bmatrix} Q_{H1}(t-0.5) \\ Q_{T1}(t-0.5) \end{bmatrix} + \begin{bmatrix} L_H\alpha_H\theta_A(t-0.5) \\ -\alpha_T D_{T1}(t-0.5) \end{bmatrix}$$

$$\begin{bmatrix} \theta_{H2}(t) \\ \theta_{T2}(t) \end{bmatrix} = \begin{bmatrix} \mu_H & 0 \\ L_T\alpha_T & \mu_T \end{bmatrix} \begin{bmatrix} \theta_{H2}(t-0.5) \\ \theta_{T2}(t-0.5) \end{bmatrix} + \begin{bmatrix} \alpha_H & 0 \\ 0 & \alpha_T \end{bmatrix} \begin{bmatrix} Q_{H2}(t-0.5) \\ Q_{T2}(t-0.5) \end{bmatrix} + \begin{bmatrix} L_H\alpha_H\theta_A(t-0.5) \\ -\alpha_T D_{T2}(t-0.5) \end{bmatrix}$$

$$Q_{H1}(t) + Q_{T1}(t) + Q_{H2}(t) + Q_{T2}(t) = \eta_{th} Q_{CHP}(t) + \eta_b Q_{Boiler}$$

Bounds:

1. Temperature constraints

$$\begin{bmatrix} \theta_{H,ref,\min} \\ \theta_{T,ref,\min} \end{bmatrix} \leq \begin{bmatrix} \theta_{H1}(t) \\ \theta_{T1}(t) \end{bmatrix} < \begin{bmatrix} \theta_{H,ref,\max} \\ \theta_{T,ref,\max} \end{bmatrix}$$

$$\begin{bmatrix} \theta_{H,ref,\min} \\ \theta_{T,ref,\min} \end{bmatrix} \leq \begin{bmatrix} \theta_{H2}(t) \\ \theta_{T2}(t) \end{bmatrix} < \begin{bmatrix} \theta_{H,ref,\max} \\ \theta_{T,ref,\max} \end{bmatrix}$$

The minimum and maximum bounds for space and hot water temperatures were defined to represent seasonal variations and the comfort of residents.

2. Capacity constraints

$$Q_{CHP}(t) = \begin{cases} 7\text{ kW when uCHP is ON} \\ 0 \quad \text{when uCHP is OFF} \end{cases}$$

$$Q_{Boiler}(t) \leq 10kW$$

### (b) Economic consideration for different occupancy patterns

In order to assess the cost benefits that can be achieved by the different occupancy patterns of each house, the occupancy patterns given in Table 10 were considered.

Table 9: Occupancy patterns of residents

| Pattern | Type of Behaviour |
|---|---|
| 1 | Not working |
| 2 | Part-time working morning (9.00 to 13.00) |
| 3 | Full-time working |

The reference setting of the inside temperature of the house, hot water temperature, hot water demand and electricity demand given in Appendix A were shifted to account for different occupancy patterns and are shown in Appendix B.

The total cost of gas and electricity was optimised for the occupancy patterns given in Table 10. The total cost of gas and electricity for different combinations of occupancy patterns is given in Table 11 The table compares the total cost for a separate µCHP unit in each house and for an interconnected µCHP unit with a boiler supplying both houses.

Table 10: The cost of electricity and gas when gas price is 2 pence per kWh

| Combination of occupancy patterns in houses 1 and 2 | Two uCHP units | | Interconnected uCHP and a Boiler £/day |
|---|---|---|---|
| | Without selling £/day | With selling £/day | |
| 1 - 1 | 4.68 | 4.60 | 4.62 |
| 1 - 2 | 4.73 | 4.65 | 4.61 |
| 1 - 3 | 4.69 | 4.62 | 4.61 |
| 2 - 2 | 4.78 | 4.70 | 4.64 |
| 2 - 3 | 4.74 | 4.67 | 4.61 |
| 3 - 3 | 4.70 | 4.64 | 4.57 |

Figure 27 shows the utilisation of the µCHP unit and the boiler. In all cases, except for the case where both houses have the occupancy patterns 1-1 and 3-3, the utilisation of the boiler is negligible. This indicated that if the two houses are willing to compromise on comfort for one and half hour around 5:30 am or 8.00 am (house and hot water temperature were maintained at 20°C and 50°C during this period), the µCHP unit can supply the thermal requirement of both houses. For all combinations of occupancy patterns the electricity generated from the µCHP unit is consumed within the two houses.

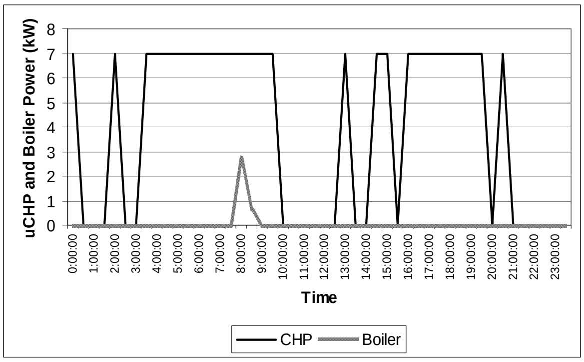


(a) For occupancy pattern 1 - 1

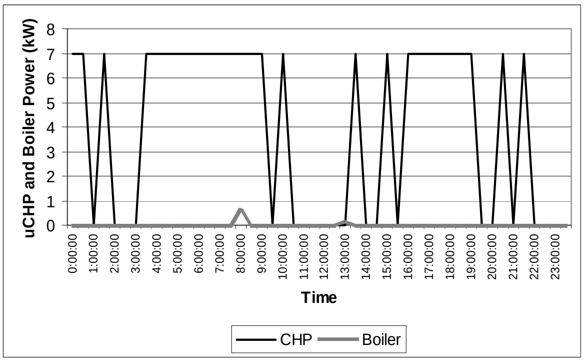


(b) For occupancy pattern 1 - 2

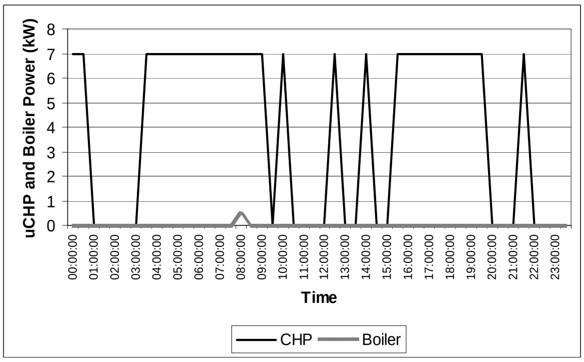


(c) For occupancy pattern 1 - 3

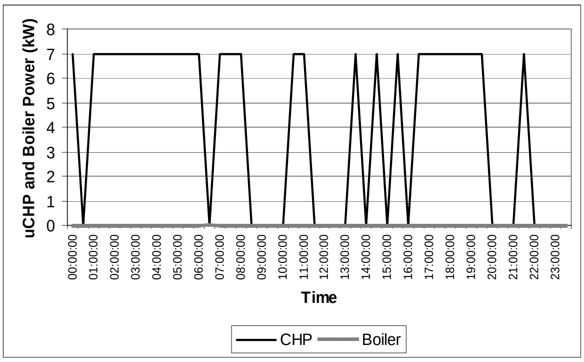


(d) For occupancy pattern 2 - 2

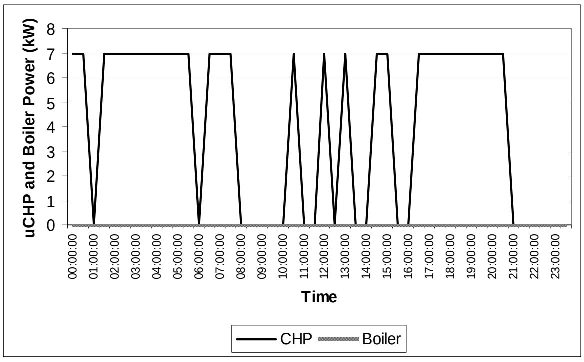


(e) For occupancy pattern 2 - 3

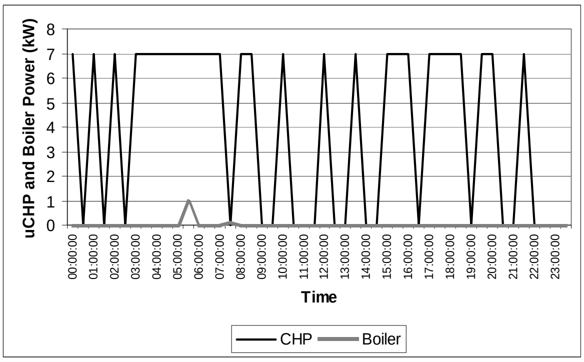


(f) For occupancy pattern 3 - 3

Figure 27: uCHP and Boiler output power

## 4.8 Conclusions

Two control strategies one based on temperature control and the other based on cost minimisation while maintaining the space and hot water temperature within maximum and minimum bounds were considered for a house with a µCHP unit. The µCHP considered was one which operates in full-load and idling (or off) mode where switching on and off times were based on the reference temperature setting of the dwelling. It was shown that a cost reduction can be achieved if the µCHP unit was controlled in optimum cost controlled mode but this level of cost reduction (£50-60/year) may not justify the expense of the control system required. Further cost reductions can be achieved if provisions exist to sell electricity to the grid. However, the attractiveness of selling electricity to the grid depends on the export price for electricity and on the amount of surplus energy available from the µCHP unit which varies daily and seasonally. Additionally, selling electricity to the grid will incur costs associated with the installation of bi-directional meters at each dwelling. It was estimated that when the µCHP is operating on the cost controlled mode, the electricity that is generated and utilised locally amounts to 1836 kWh per year per household. This is equivalent to 0.56 T to 0.73 T of CO2 savings per household per year.

The cost optimisation model was extended to incorporate a µCHP unit which is connected to two semi-detached houses where both electrical and thermal systems are interconnected. It was shown that the optimum cost operation of a µCHP is maximised if each dwelling has a different occupancy pattern. The cost reduction was greater than that can be obtained for two µCHP units connected individually in each house even with the provision for selling electricity to the grid. Except in the cases where the occupants of both houses are not working or in full time work, a single µCHP can fulfil the heat requirement of both houses thus giving further cost reduction in terms of capital cost. The use of a single µCHP unit to serve two houses (larger load) results in maximising the utilisation of the unit and minimising cycling on and off times. However, the practical implementation of such a scheme requires additional costs related to electricity and heat metering at both dwellings.

*Chapter 5*

# HOUSING ESTATE WITH µCHP UNIT FOR POWER FLOW STUDIES

## 5.1 State space model of an individual house

The thermal model of a house given in equation (1.5) can be represented by a state space model as follows:

$$x_{i+1} = Ax_i + Bu_i + Hd_i \tag{5.1}$$

Where $x_{i+1} = \begin{bmatrix} \theta_H(i+1) \\ \theta_T(i+1) \end{bmatrix}$, $x_i = \begin{bmatrix} \theta_H(i) \\ \theta_T(i) \end{bmatrix}$, $u_i = \begin{bmatrix} Q_H \\ Q_T \end{bmatrix}$, and $d_i = \begin{bmatrix} \theta_A \\ D_T \end{bmatrix}$

$$A = \begin{bmatrix} \mu_H & 0 \\ L_T\alpha_T & \mu_T \end{bmatrix}, \quad B = \begin{bmatrix} \alpha_H & 0 \\ 0 & \alpha_T \end{bmatrix}, \text{ and } H = \begin{bmatrix} L_H\alpha_H & 0 \\ 0 & -\alpha_T \end{bmatrix}$$

The temperature error is defined as:

$$\boldsymbol{\varepsilon} = \mathbf{y}^{ref} - \mathbf{y}$$

Where $y = \begin{bmatrix} \theta_H(i) \\ \theta_T(i) \end{bmatrix}$ and $y^{ref} = \begin{bmatrix} \theta_{H,ref} \\ \theta_{T,ref} \end{bmatrix}$

The control function defined in equation (4.1) and Figure 22 can be expressed as:

$$u_i = Q_H + Q_T = \begin{cases} \eta_{th} Q_{CHP} & \text{if } \varepsilon > \Delta\theta \text{ and } u_{i-1} = 0 \\ 0 & \text{if } \varepsilon < -\Delta\theta \text{ and } u_{i-1} = Q_{CHP} \end{cases} \tag{5.2}$$

Where $\Delta\theta$ is a dead band used for control.

Using equations (5.1) and (5.2) the state space thermal model of the house with a µCHP on a temperature control was derived and shown in Figure 28.

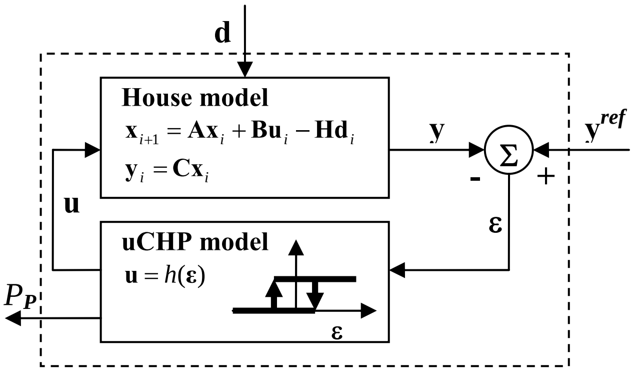


Figure 28: Thermal model of a house

The complete model of the house consists of thermal and electrical models. The electrical model is described by electricity demand $P_D$, and electrical power produced by the µCHP unit $P_P$. The Complete House Model (CHM) is shown in Figure 29.

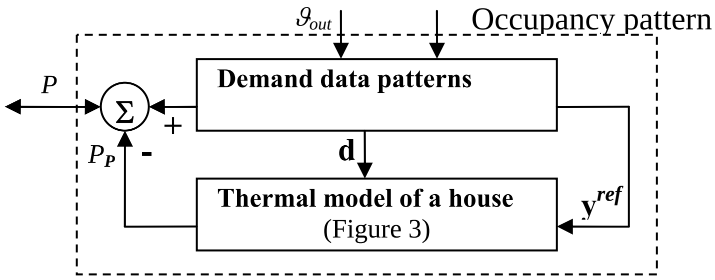


Figure 29: Complete house model (CHM)

## 5.2 Model of an estate of houses

An estate consists of a number of houses, N, connected to a single feeder was considered. Each house was represented by a CHM shown in Figure 29. Since the estate lies in the same geographical area, it was assumed that each $CHM_k$ model is subjected to the same outside temperature $\theta_A$. The houses in the estate were categorised under the occupancy patterns shown in Table 11 [4]. Assuming there are $sc_i$ (i = 1…n) number of houses under each category (percentage value is given in Table 11), the model for the estate was derived and shown in Figure 30. A simple representation of the electrical distribution network was used. The network was represented by a single bus bar model where distribution losses were neglected.

Electrical power flow through a feeder was calculated by adding the sum of power flows of individual houses.

Table 11: Occupancy patterns in the estate and no. of houses under each category.

| Occupancy Pattern | Type of behaviour | Unoccupied period | No of houses in each category [ % ] |
|---|---|---|---|
| 1 | Part time working morning | 9:00 to 13:00 | 25 |
| 2 | Complete time working | 9:00 to 18:00 | 30 |
| 3 | Part time working | 9:00 to 16:00 | 25 |
| 4 | No working | N/A | 7 |
| 5 | Part time working afternoon | 13:00 to 18:00 | 13 |

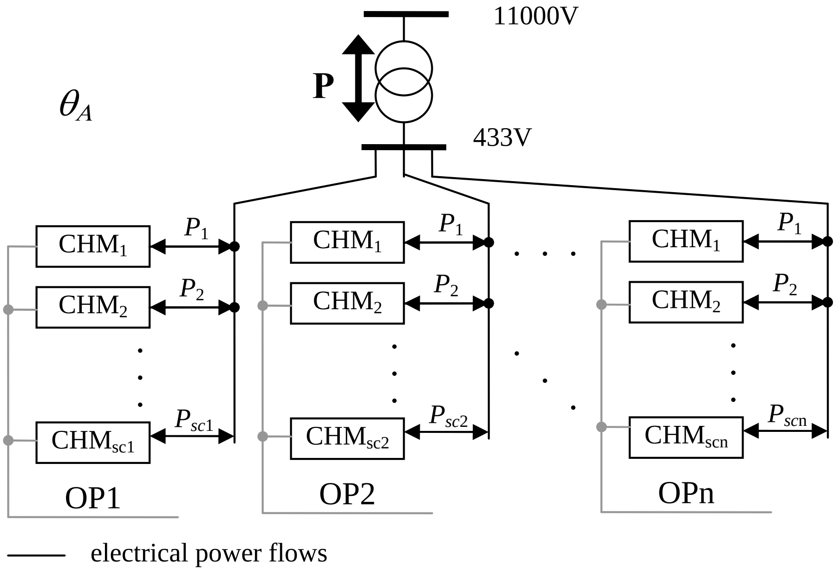


Figure 30: Estate model

## 5.3 Results of simulations

It was assumed that there are 150 houses in the estate and each house was equipped with a Stirling engine type μCHP unit, with rated power of $7kW_{th}$ for flats and $10kW_{th}$ for semi-detached houses. The thermal and electrical efficiencies of the μCHP were assumed as 80% and 10% respectively.

The hot water demand and electrical demand under different occupancy patterns were determined on the basis of hourly data given in [4]. It was assumed that the hot water usage is described by random peak demands for the period of simulations while maintaining average hourly consumption. The heating periods, human heat gains and set point reference signals were constructed on the basis of occupation periods given in Table 11. For example for occupancy pattern 1, there are two heating periods: 5:00–8:00 and 13:00–21:00, for occupancy pattern 2 heating periods: 5:00–8:00 and 17:00–21:30 and so on. Outside temperature data was based on a CIBSE Met Office Hourly Weather Data for North West region, UK [11]. Because demand and temperature data were provided with 1 hour time intervals, it was assumed that linear changes occurred between each time step used for simulations.

## (a) Results for an Individual house

The CHM given in Figure 29 was simulated to control the temperature inside the house and hot water temperature towards two references. The data used for the flat and semi-detached house is given in Appendix C. The space and hot water temperatures with their respective reference temperatures, hot water demand and $u_i = Q_H + Q_T$ for the µCHP for winter, summer and spring/autumn is shown in Figure 31. In that figure, the hot water demand and $u_i$ were scaled. The highest daily hot water demand was also shown in the figure. The maximum value of $u_i$ was the rated power of the µCHP unit.

During the time the µCHP is ON, the hot water temperature, $\theta_T$, increases and falls during the time the µCHP is OFF. The fall in hot water temperature was mostly affected by hot water demand. Losses were not significant for the parameters chosen for HWT, so it was difficult to observe them.

The fall of house temperature, $\theta_H$, was mostly affected by heat losses. This can be seen by the comparison of winter and summer results. For winter especially $\theta_H$ oscillated close to $\theta_{H,ref}$. For summer, with few exceptions $\theta_H > \theta_{H,ref}$, and very little space heating was needed.

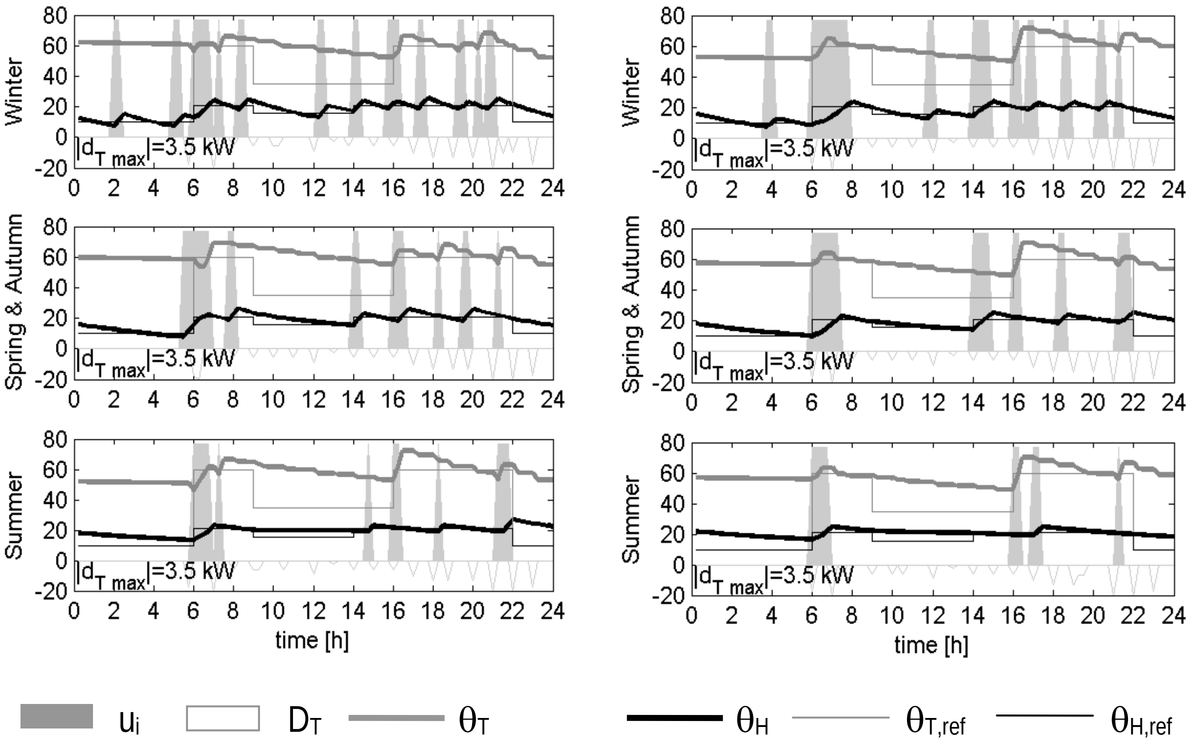


(a) For a flat (b) semi-detached house

Figure 31: Thermal dynamics of an individual house with heat demand control for different seasons of a year for occupancy pattern 1; $d_T$ and $u$ scaled. $u_{max} = P_{rated}$

## (b) Estate: µCHP switching patterns

The Estate model shown in shown in Figure 30 was used for these simulations. Two estates one with 150 flats and the other with 150 semi-detached houses were considered for this study. Each estate was modelled for different seasons of a year. Depending on the occupancy pattern, each house was controlled to maintain the space and hot water temperatures towards the references. The µCHP switching patterns required to maintain the reference temperatures for every house in the estate are shown in Figure 32. The switching patterns were divided into groups. Each group was represented by an occupancy pattern. Each row represents the behaviour of a µCHP unit in an individual house. Line (—) represent the ON state of a unit.

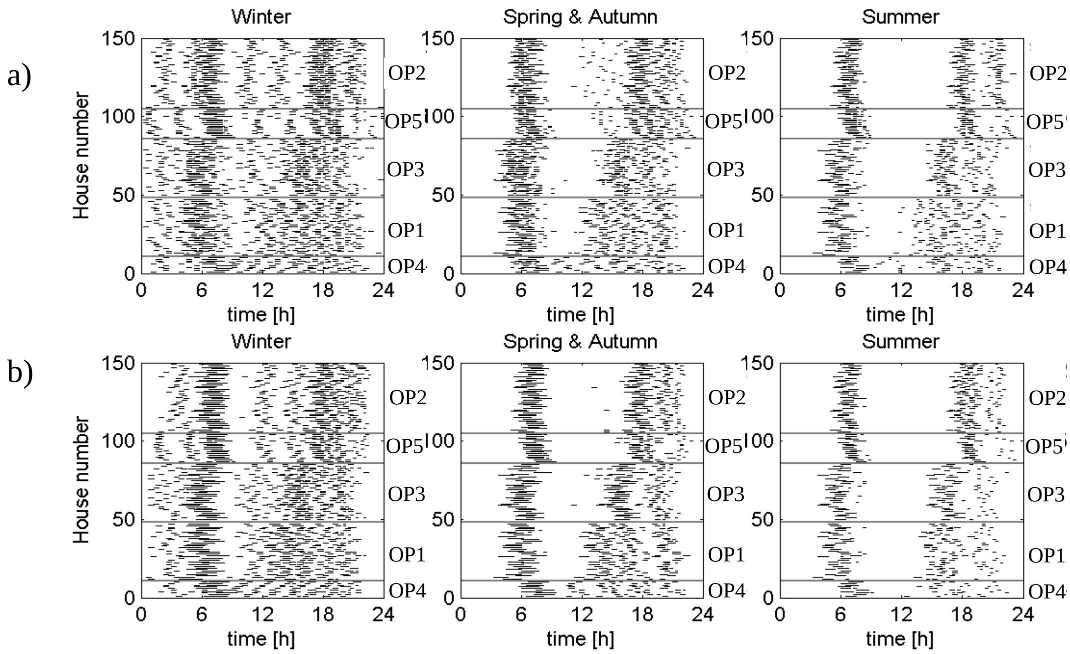


Figure 32: μCHP switching patterns for different estates, scenarios and weather conditions a) flats, b) semi-detached houses.

The heating periods with temperatures for space heating and hot water are shown in Figure 33 for both estate models (flats and semi-detached houses). The heating periods with temperatures and set point reference signals were also divided into groups based on the occupancy pattern. Each row represents an individual house reference. Line lengths represent the duration of heating.

During summer, the switching patterns were influenced by the HWT temperature references only. This is seen by comparing the summer switching patterns (Figure 32) with space heating and HWTs references (Figure 33). There is a period in the day when only space heating was requested (Figure 33, between 9 a.m. and 3 p.m., Occupancy patterns 1 and 4).There was no heat/electricity production during this period in the summer (Figure 32). The μCHP units were switched around 3 p.m. due to the demand for hot water.

During spring and autumn the switching patterns were influenced by space heating and HWTs references. Spring and autumn switching patterns visibly reflect space heating references. Switching caused by HWTs references was integrated.

During winter the switching patterns were mainly influenced by space heating references. This is seen mainly by switching patterns which occur between heating periods, and in the night.

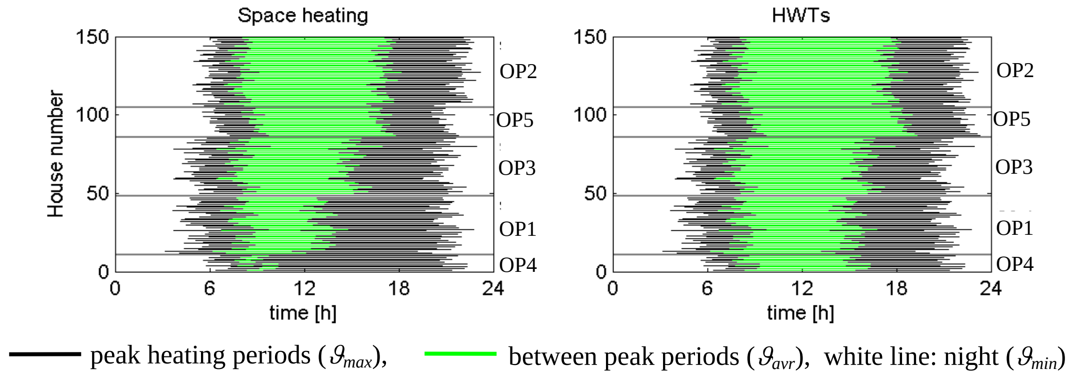


Figure 33: Heating periods with temperatures for space heating and HWTs for occupancy patters

## (c) Estate: electrical power flows

Results of electrical power flows for different estates are shown in Figure 34. Figure 34(a) shows an estate with flats and Figure 34(b) shows an estate with semi-detached houses.

Power generation $P_P$, as well as power demand $P_D$ was affected by temperature changes, and this is clearly seen in Figure 34. The difference in generation between the two estates was mostly affected by heat demand, which was bigger for semi-detached houses. There was a 30% peak difference in electricity generation during early morning hours, in winter. During summer there was no difference, because generation was affected by hot water demand, which was similar for both estates.

As a result of electrical power demand $P_D$ and power generation $P_P$, electrical power flow into the grid through a feeder P was obtained (Figure 30). It was possible to observe reverse power flows for both estates. The longest period occurred during winter and lasted 4-5 hours (early morning).

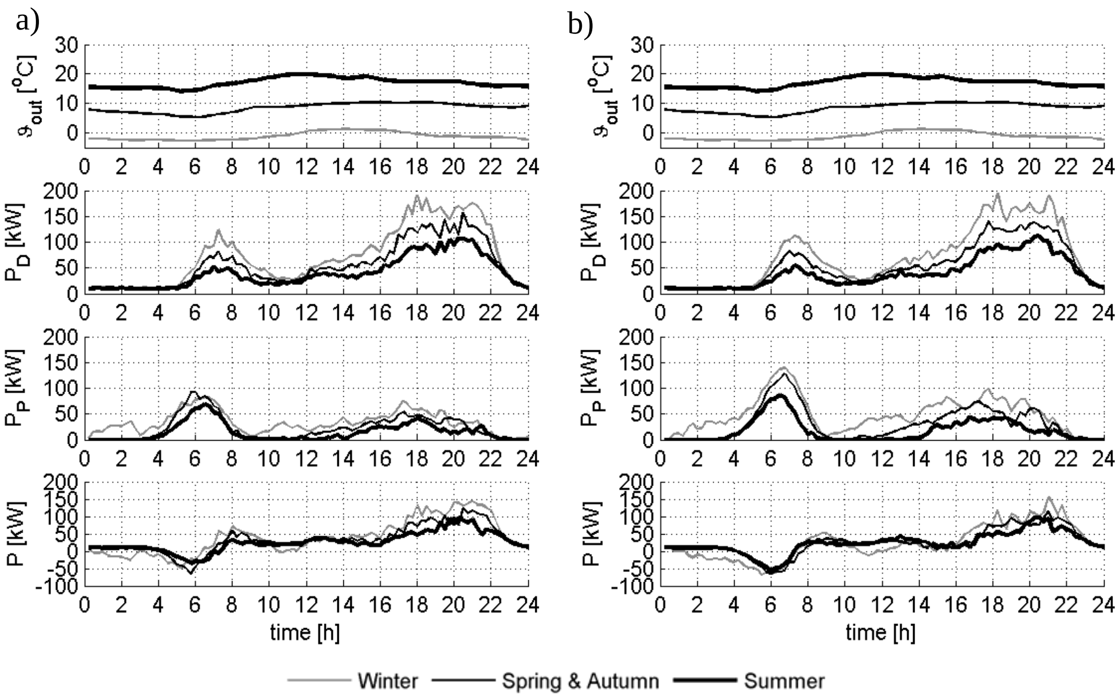


Figure 34: Electrical power flows for different estates a) flats, b) semi-detached houses

## 5.4 Conclusions

### (a) House thermal model

The model of a house was an approximate representation of a real dwelling, but took important elements into account. These were house structure and HWT, hot water demand and behaviour of residents. The parameters of the house combined with outside temperature and heating periods gave the thermal dynamics of a house. The parameters of the HWT combined with hot water demand and periods of heating gave the thermal dynamics of the hot water tank. These elements together formed a useful model, to determine the behaviour of µCHP units (its switching pattern) as a result of outside temperature changes, and residents' behaviour.

### (b) Estate model

The estate model was represented by outside temperature $\theta_A$ and percentage of residents' behaviour patterns. Such a model can be used in electrical load flow studies.

To represent such an estate the Distribution Network Operator (DNO) should take account of the ambient temperature, and have a basic knowledge of residents' behaviour. This is important in the case of a rapid fall in outside temperature, which affects, with some delay, the generation of electricity (because of higher heat losses in the houses). The response would be much faster if the fall is deeper, or initial outside temperature is lower.

# REFERENCES


1. *Meeting the Energy Challenge a White Paper on Energy*, U. Department of Trade and Industry, Editor. May 2007.

2. Harrison, J. and S. Redford, *Domestic CHP: What are the potential benefits?* June 2001, EA Technology Ltd, Accessed 20/01/2008, http://www.whispergen.com/content/library/ESTbenefits.pdf.

3. Pudjianto, D. and G. Strbac, *Methodology for Quantifying Economic and Environmental Benefits of MicroGrids* in *Large Scale Integration of Micro-Generation to Low Voltage Grids - Work package G*. July 2005: The University of Manchester.

4. Steemers, K. and R. Yao, *Microgrids - Distributed On-site Generation*, in *Working Package – Modelling Of Energy Consumption in Building*. May 2003, Department of Architecture Report, University of Cambridge.

5. Abu-Sharkh, S., et al. March 2005, Tyndall Centre report No 22.

6. Geidl, M. and G. Andersson, *Optimal power dispatch and conversion in systems with multiple energy carriers*, in *15th Power Systems Computation Conference*. 2005: Liege, Belgium.

7. *Switch with confidence*. [Cited 20/01/2008]; Available from: http://www.uswitch.com.

8. Walsh, G.R., *Methods of Optimization*. 1985: John Wiley & Sons Ltd.

9. Wood, A.J. and B.F. Wollenberg, *Power generation, operation, and control*. 1996: John Wiley & Sons Ltd.

10. *Dash Xpress optimisation*. [Cited 20/01/2008]; Available from: http://www.dashoptimization.com/.

11. *CIBSE/Met Office TRY/DSY Hourly Weather Data Set*. [Cited 29/11/2007]; Available from: http://www.cibse.org/index.cfm?go=publications.view&PubID=332&S1=y&L1=0&L2=0.

12. *Demand Data*. [Cited 08/11/2007]; Available from: http://www.nationalgrid.com/uk/Electricity/Data/Demand+Data/.

# APPENDIX A

## 1. Electricity demand [5]

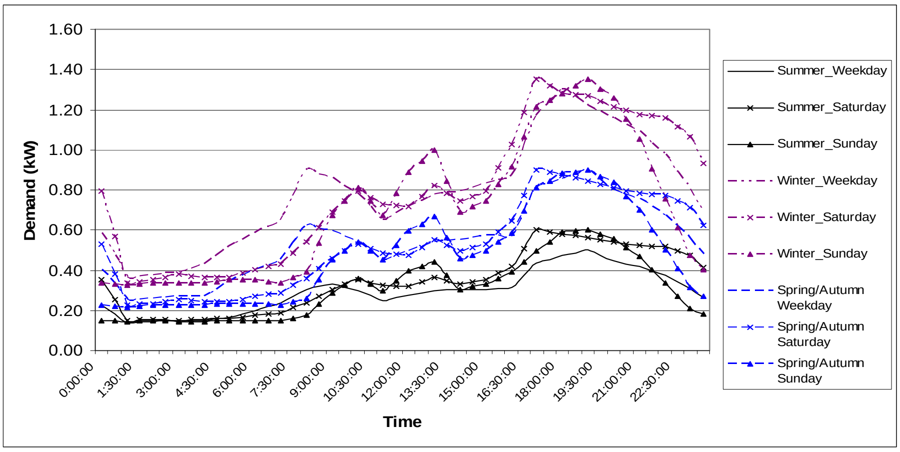


Figure A1: Electricity demand profiles

## 2. Hot water demand [5]

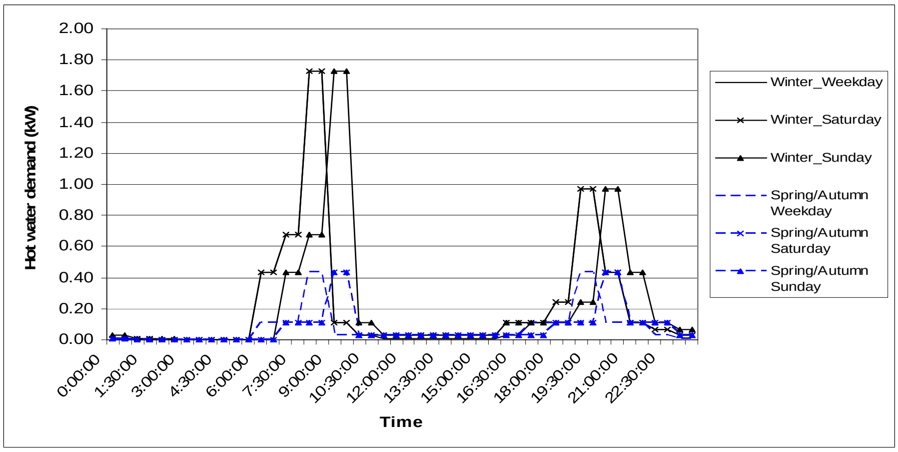


Figure A2: Hot water demand profiles

3. Outside temperature – typical temperature profile was assumed.

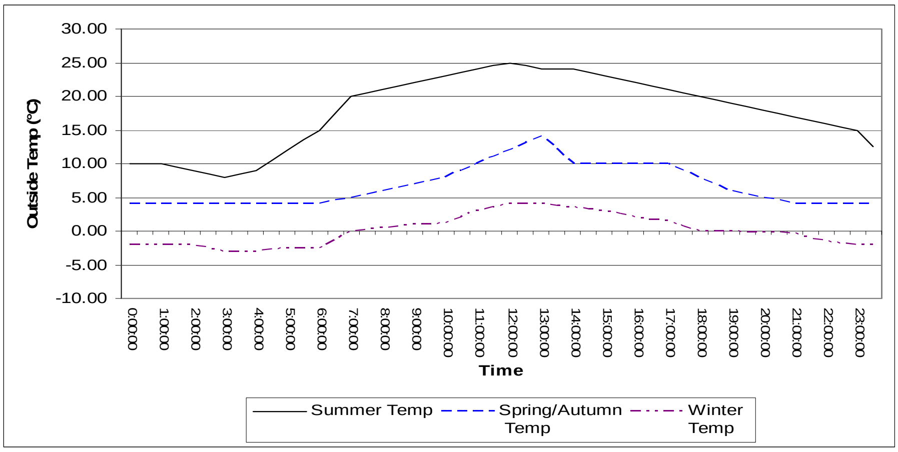


Figure A3: Outside temperature profiles

4. Electricity prices – It was assumed that the electricity price is varying with the electricity demand with an average of 10 pence per kWh [12].

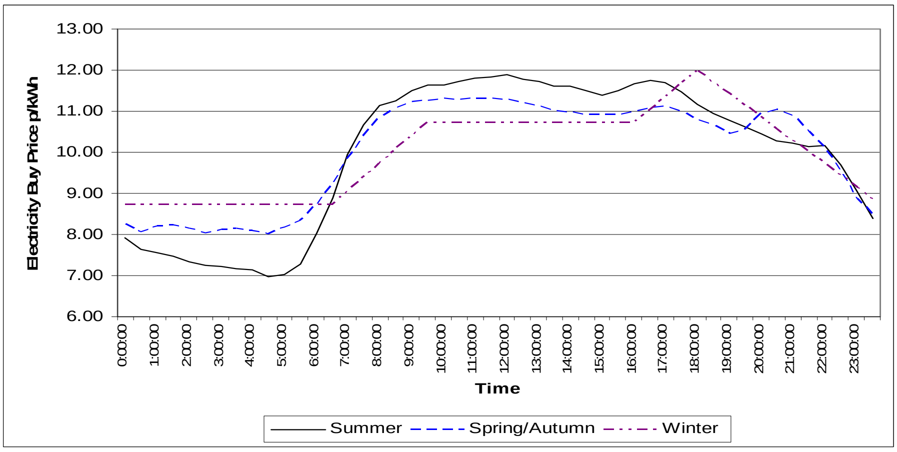


Figure A4: Electricity prices

# APPENDIX B

1. Electricity demand

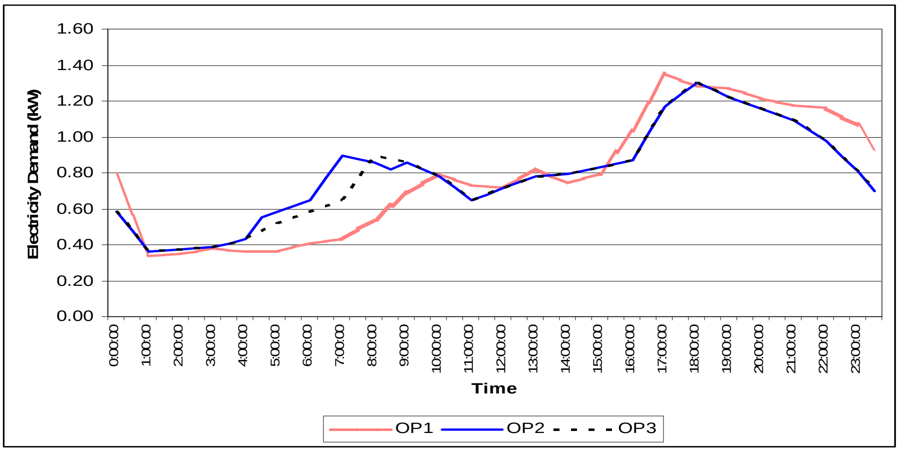


Figure B1: Electricity demand profiles

2. Hot water demand

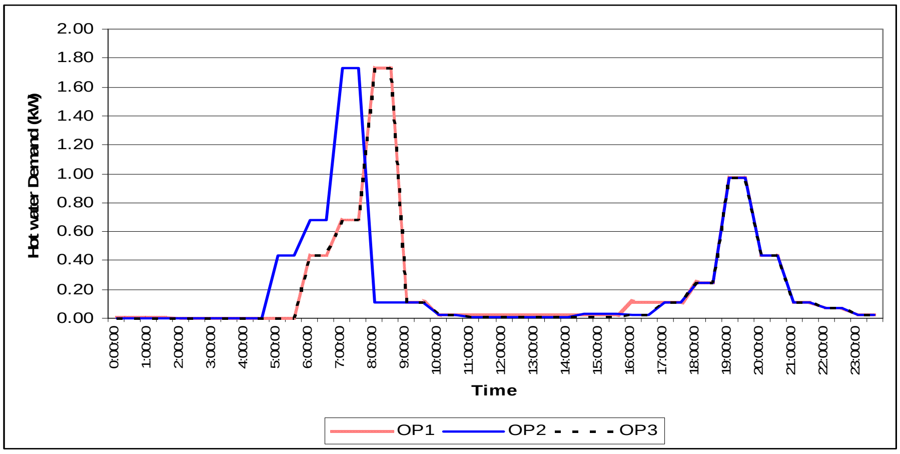


Figure B2: Hot water demand profiles

3. Temperature reference for the house

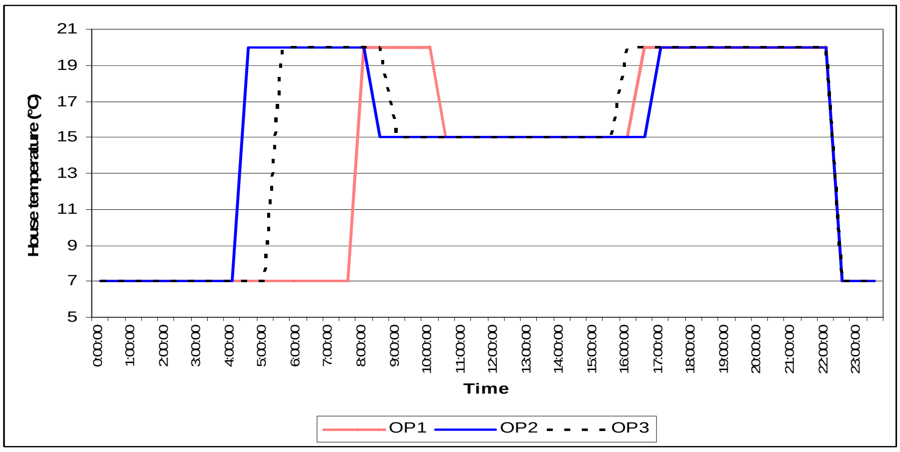


Figure B3: Outside temperature profiles

4. Temperature reference for hot water.

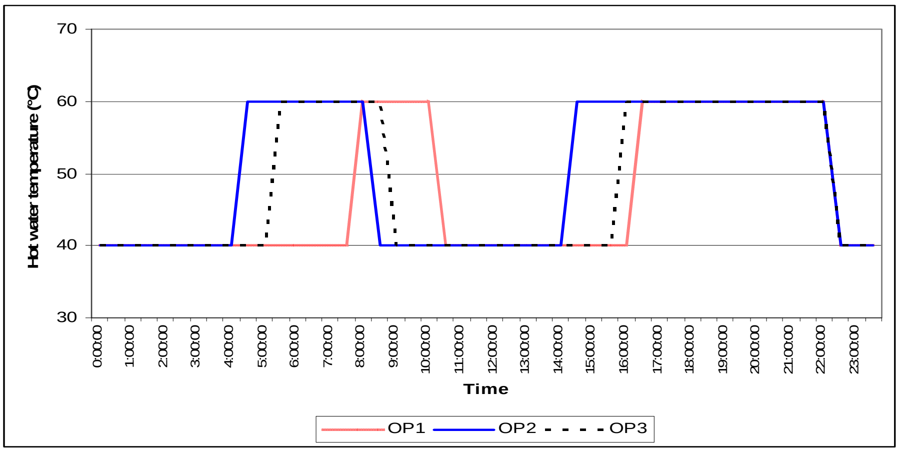


Figure B4: Electricity prices

# APPENDIX C

## C1 House structure

Parameters of the house are shown in Table C1.

Table C1: Parameters for different types of house structures.

| | House parameters | |
|---|---|---|
| Type of a house structure | capacity: C [kWh/K] | losses: L [kW/K] |
| Flat | 0.4032 | 0.0669 |
| Semi detached house | 0.8064 | 0.1130 |

## C.2 HWT

Parameters of a HWT were calculated on the basis of its physical properties: capacity, shape (area of heat radiation), thickness and resistivity of insulation. HWT was represented by volume (V) and thermal resistance (R-value). Parameters are shown in Table C2. Bigger HWT was used for a semi detached house, smaller for a flat.

Table C2: Parameters for different HWTs.

| Tank | | House parameters | |
|---|---|---|---|
| V [$dm^3$] | R-value [$Km^2/W$] | capacity: C [kWh/K] | losses: L [kW/K] |
| 150 | 5 | 0.1680 | 0.0003 |
| 200 | 5 | 0.2240 | 0.0004 |